Phase Behavior

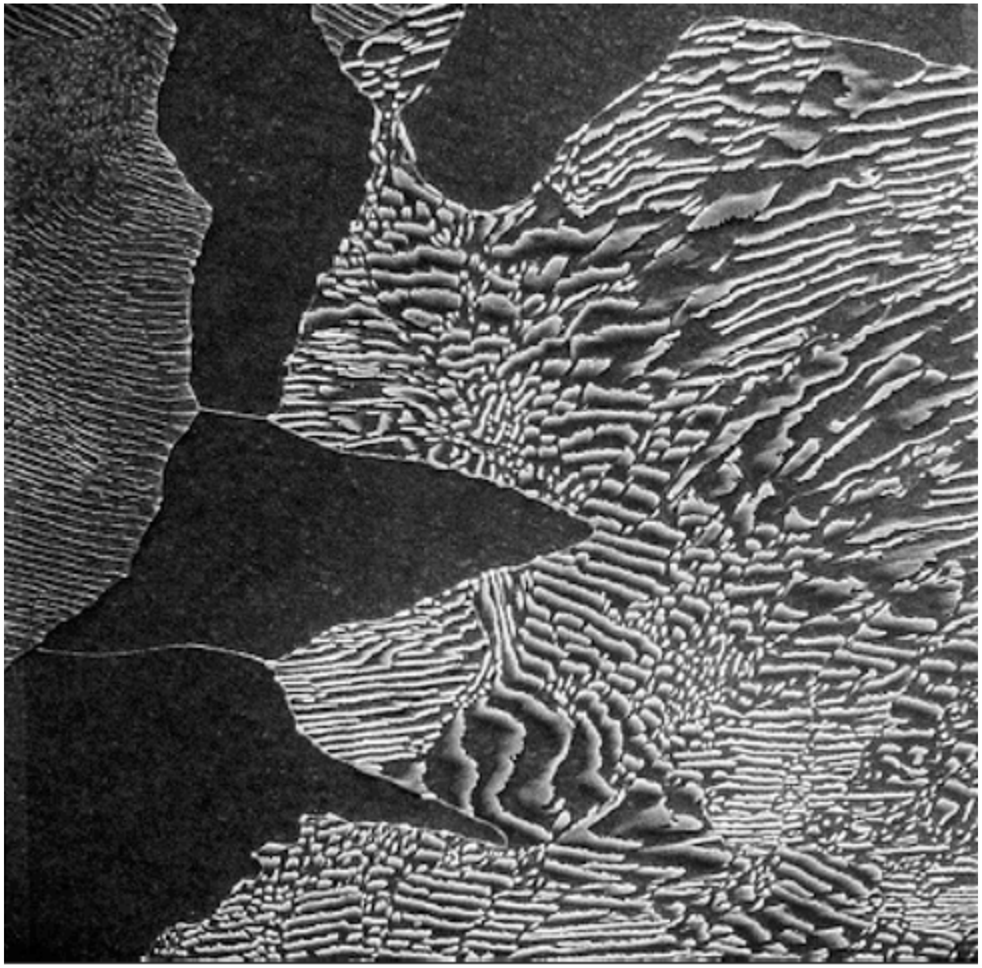

Callister P. 252
Chapter 9

A scanning electron micrograph showing the microstructure of a plain carbon steel that contains 0.44 wt% C. The large dark areas are proeutectoid ferrite. Regions having the alternating light and dark lamellar structure are pearlite; the dark and light layers in the pearlite correspond, respectively, to ferrite and cementite phases. During etching of the surface prior to examination, the ferrite phase was preferentially dissolved; thus, the pearlite appears in topographical relief with cementite layers being elevated above the ferrite layers. 3000×. (Micrograph courtesy of Republic Steel Corporation.)

Chalcolithic Era (7000 BC)
(Copper Working)

Bronze Age
Copper and Arsenic (3000 BC)
Ores from same site

or Copper and Tin “Alloys” (2000 BC times vary around world)
Coincident Ores in Thailand others involve trade
(UK source of Tin)

Iron Age
Cast Iron

Steel (Iron & Carbon and Chromium Alloys) & Brass (Copper and Zinc Alloy) came later

Ideal gas mixing $$\frac{\Delta G}{kT} = \phi_A \ln(\phi_A) + \phi_B \ln(\phi_B)$$

Can be derived from the Boltzman Equation $\Delta S_{mix} = k \ln \Omega$ Ω is the number of arrangements

Flory-Huggins Equation for Polymer Blends

$$\frac{\Delta G}{kT} = \frac{\phi_A}{N_A} \ln(\phi_A) + \frac{\phi_B}{N_B} \ln(\phi_B) + \phi_A \phi_B \chi_{AB}$$

ΔG Free energy difference in going from separate polymers to mixed polymers
Φ_A Volume Fraction of polymer A
N_A Degree of polymerization (molecular weight/monomer molecular weight) of polymer A
χ_{AB} Difference between enthalpic interactions of A and B chain units alone and in blend per kT ~ 1/Temperature.

There are 3 regimes for this equation:
Single Phase,
Critical Condition,
2 Phase

Flor Huggins Equation for Polymer Blends

$$\frac{\Delta G}{kT} = \frac{\phi_A}{N_A}\ln(\phi_A) + \frac{\phi_B}{N_B}\ln(\phi_B) + \phi_A\phi_B\chi_{AB}$$

ΔG Free energy difference in going from separate polymers to mixed polymers
Φ_A Volume Fraction of polymer A
N_A Degree of polymerization (molecular weight/monomer molecular weight) of polymer A
χ_{AB} Average interaction between A and B chain units ~ 1/Temperature.

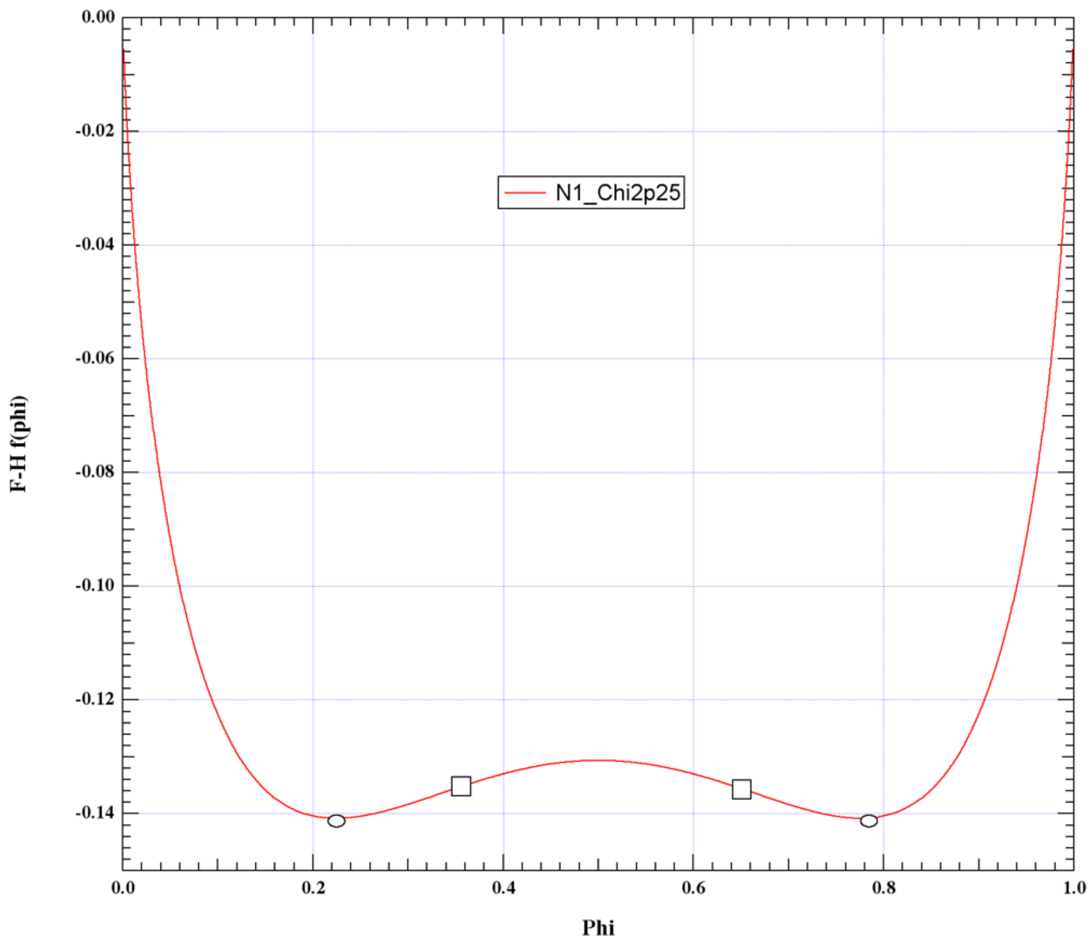

Two Phase Regime

Flor Huggins Equation for Polymer Blends

$$\frac{\Delta G}{kT} = \frac{\phi_A}{N_A}\ln(\phi_A) + \frac{\phi_B}{N_B}\ln(\phi_B) + \phi_A\phi_B\chi_{AB}$$

ΔG Free energy difference in going from separate polymers to mixed polymers
Φ_A Volume Fraction of polymer A
N_A Degree of polymerization (molecular weight/monomer molecular weight) of polymer A
χ_{AB} Average interaction between A and B chain units ~ 1/Temperature.

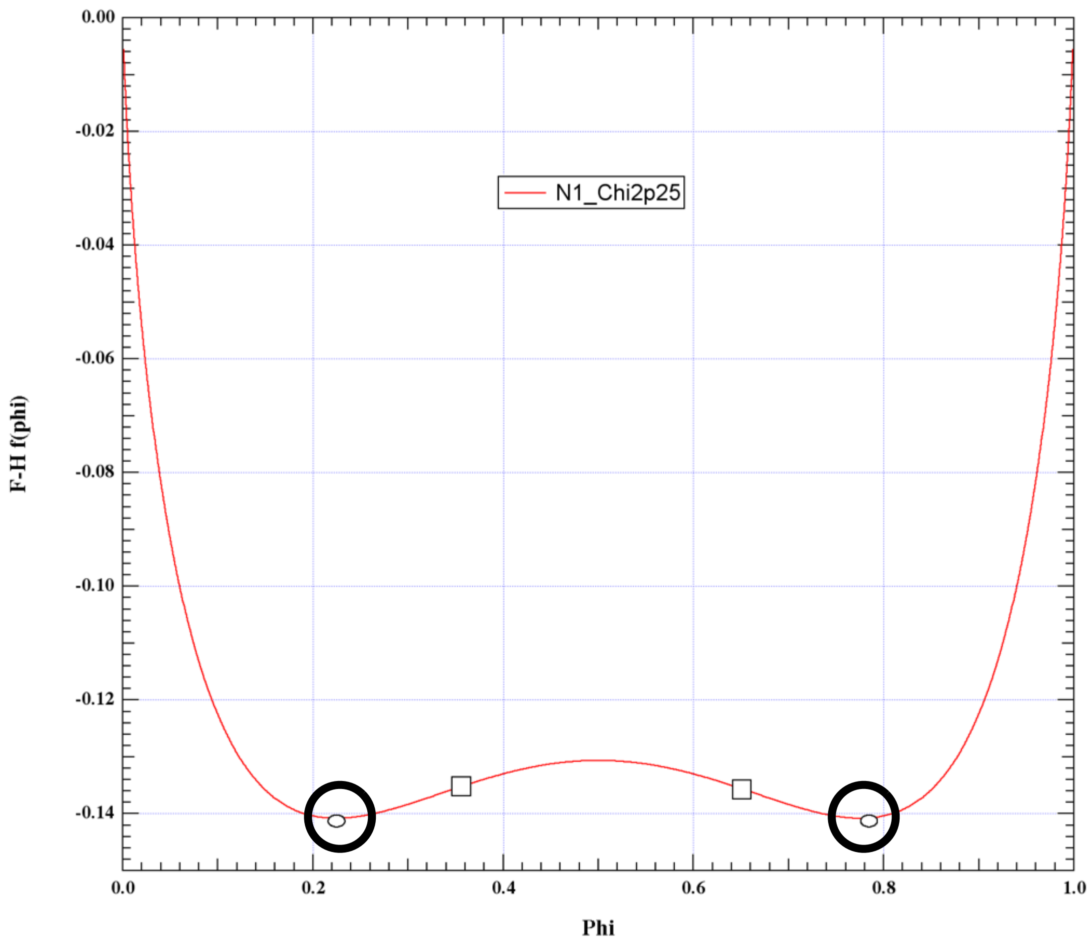

Two Phase Regime

Miscibility gap is defined by
$dG/d\Phi = \mu_A = \mu_B$

Between circles and squares
Phase Separation is an
Uphill Battle

Need a Nucleus

Nucleation and Growth

Flor Huggins Equation for Polymer Blends

$$\frac{\Delta G}{kT} = \frac{\phi_A}{N_A}\ln(\phi_A) + \frac{\phi_B}{N_B}\ln(\phi_B) + \phi_A\phi_B\chi_{AB}$$

ΔG Free energy difference in going from separate polymers to mixed polymers
Φ_A Volume Fraction of polymer A
N_A Degree of polymerization (molecular weight/monomer molecular weight) of polymer A
χ_{AB} Average interaction between A and B chain units ~ 1/Temperature.

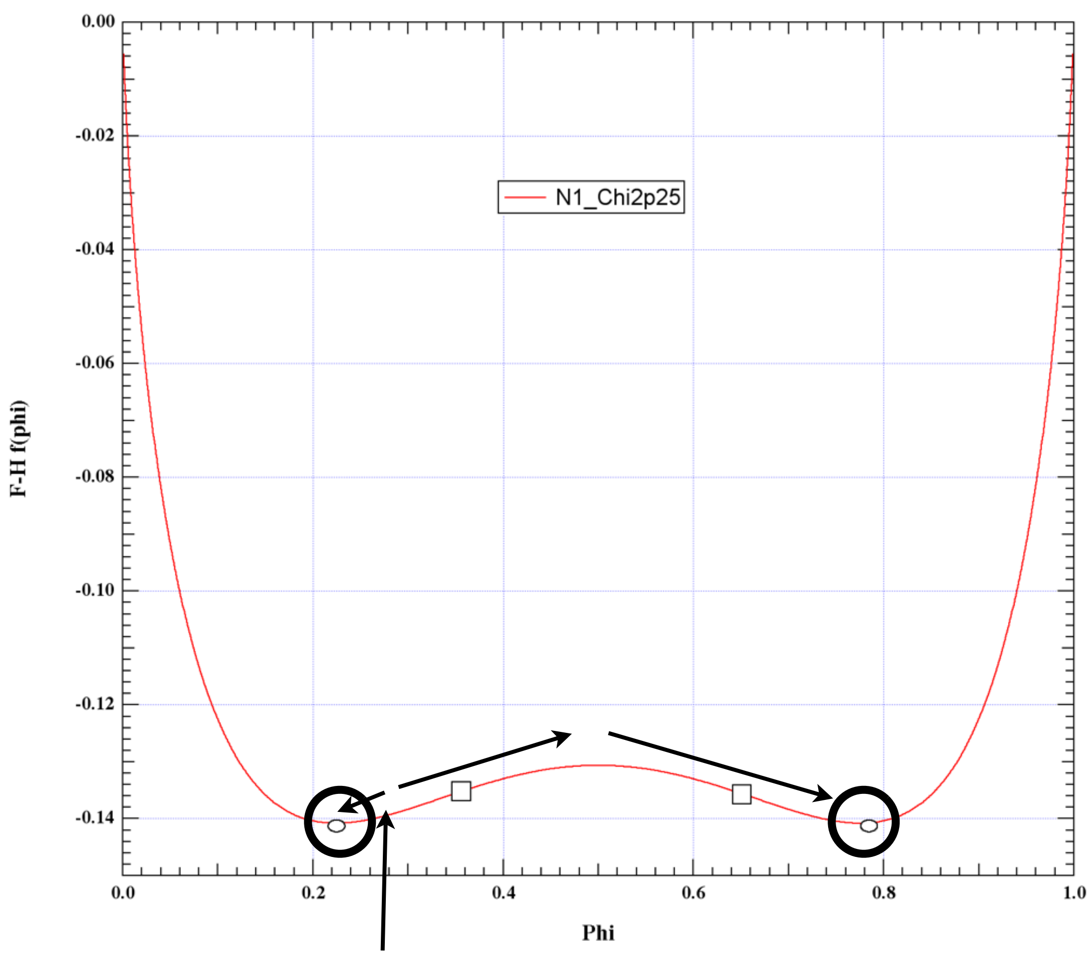

Two Phase Regime

Miscibility gap is defined by
$dG/d\Phi = \mu_A = \mu_B$

Between circles and squares
Phase Separation is an
Uphill Battle

Need a Nucleus

Nucleation and Growth

Flor Huggins Equation for Polymer Blends

$$\frac{\Delta G}{kT} = \frac{\phi_A}{N_A}\ln(\phi_A) + \frac{\phi_B}{N_B}\ln(\phi_B) + \phi_A\phi_B\chi_{AB}$$

ΔG Free energy difference in going from separate polymers to mixed polymers
Φ_A Volume Fraction of polymer A
N_A Degree of polymerization (molecular weight/monomer molecular weight) of polymer A
χ_{AB} Average interaction between A and B chain units ~ 1/Temperature.

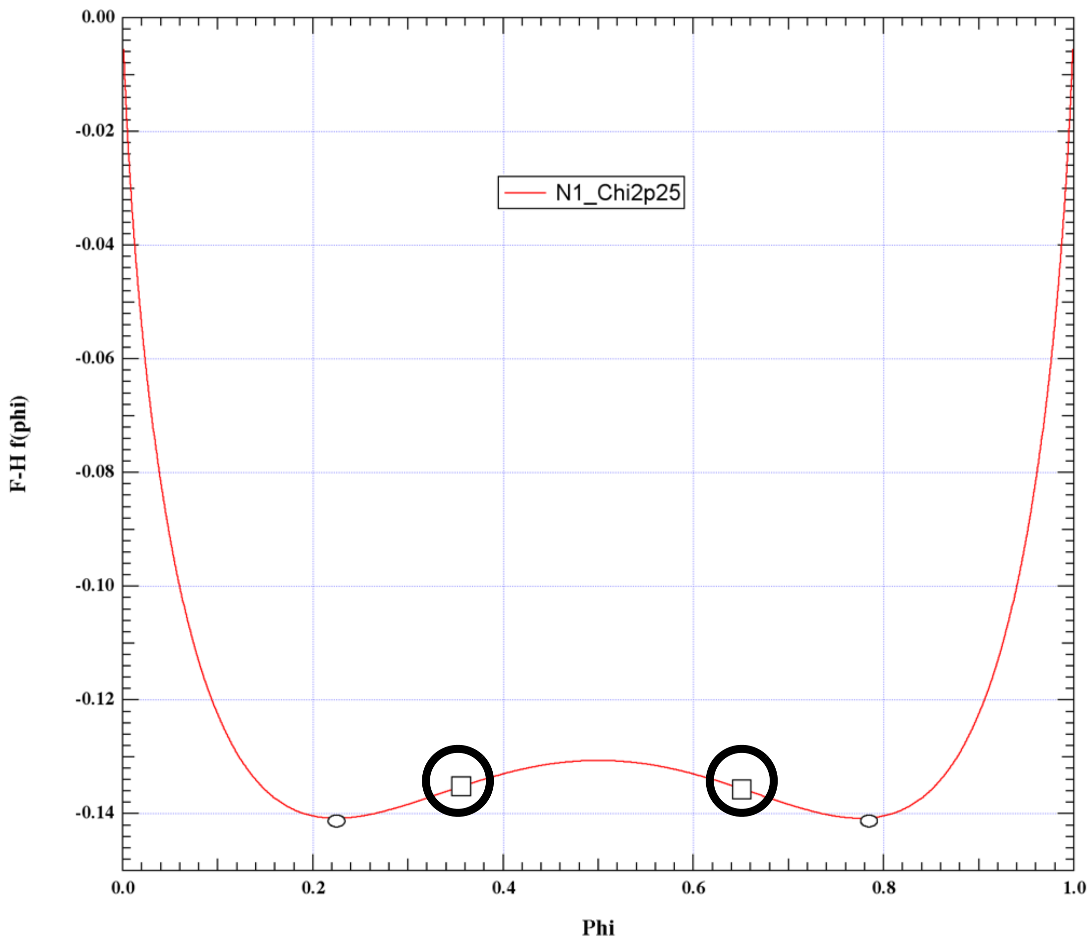

Two Phase Regime

Between squares
Phase Separation is a
Down Hill Battle

Spontaneous Phase Separation

Spinodal Decomposition

Flor Huggins Equation for Polymer Blends

$$\frac{\Delta G}{kT} = \frac{\phi_A}{N_A}\ln(\phi_A) + \frac{\phi_B}{N_B}\ln(\phi_B) + \phi_A\phi_B\chi_{AB}$$

ΔG Free energy difference in going from separate polymers to mixed polymers
Φ_A Volume Fraction of polymer A
N_A Degree of polymerization (molecular weight/monomer molecular weight) of polymer A
χ_{AB} Average interaction between A and B chain units ~ 1/Temperature.

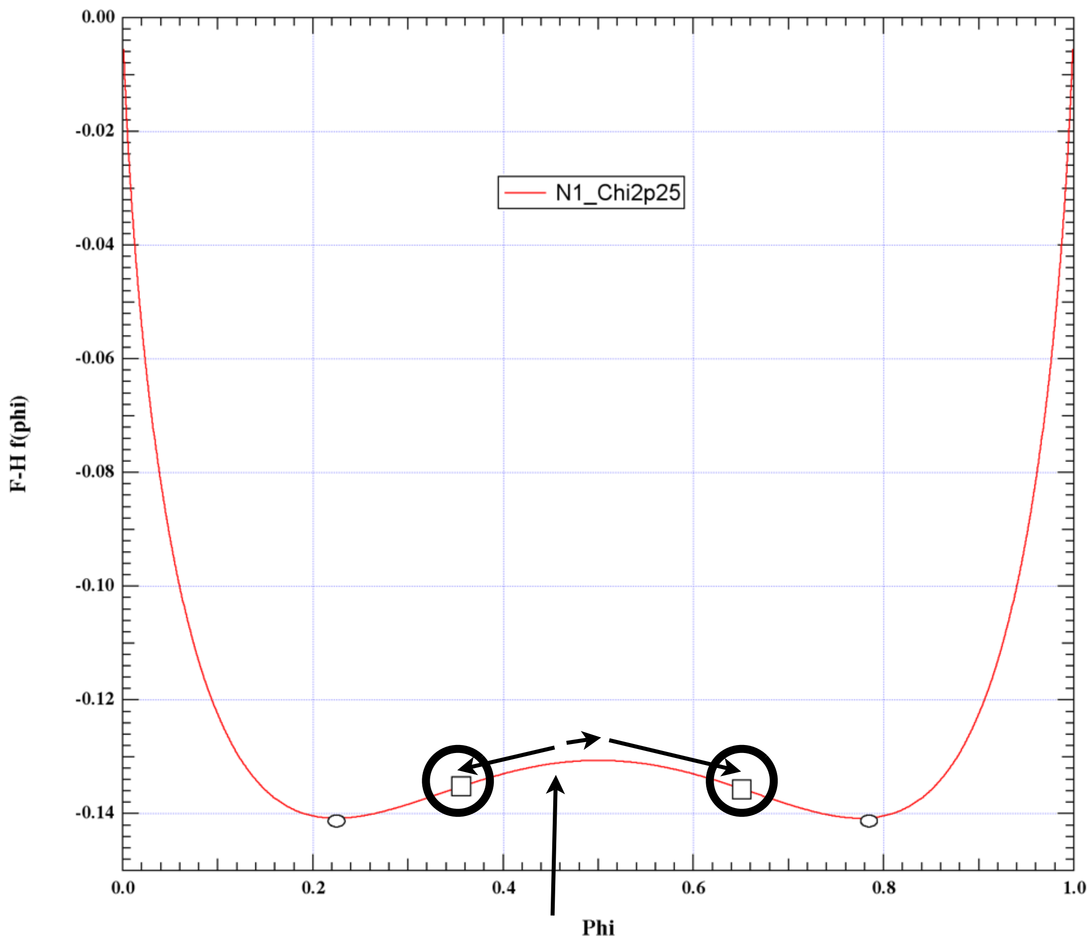

Two Phase Regime

Between squares
Phase Separation is a
Down Hill Battle

Spontaneous Phase Separation

Spinodal Decomposition

Flor Huggins Equation for Polymer Blends

$$\frac{\Delta G}{kT} = \frac{\phi_A}{N_A}\ln(\phi_A) + \frac{\phi_B}{N_B}\ln(\phi_B) + \phi_A\phi_B\chi_{AB}$$

ΔG Free energy difference in going from separate polymers to mixed polymers
Φ_A Volume Fraction of polymer A
N_A Degree of polymerization (molecular weight/monomer molecular weight) of polymer A
χ_{AB} Average interaction between A and B chain units ~ 1/Temperature.

χ_{AB}
(1/T)

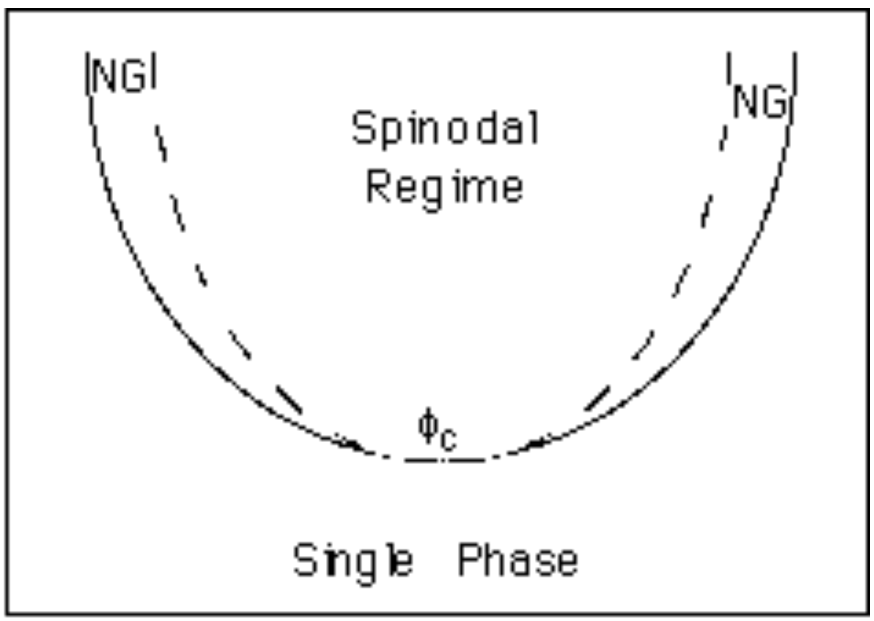

ϕ

Equilibrium Phase Diagram

Flor Huggins Equation for Polymer Blends

$$\frac{\Delta G}{kT} = \frac{\phi_A}{N_A}\ln(\phi_A) + \frac{\phi_B}{N_B}\ln(\phi_B) + \phi_A \phi_B \chi_{AB}$$

ΔG Free energy difference in going from separate polymers to mixed polymers
Φ_A Volume Fraction of polymer A
N_A Degree of polymerization (molecular weight/monomer molecular weight) of polymer A
χ_{AB} Average interaction between A and B chain units ~ 1/Temperature.

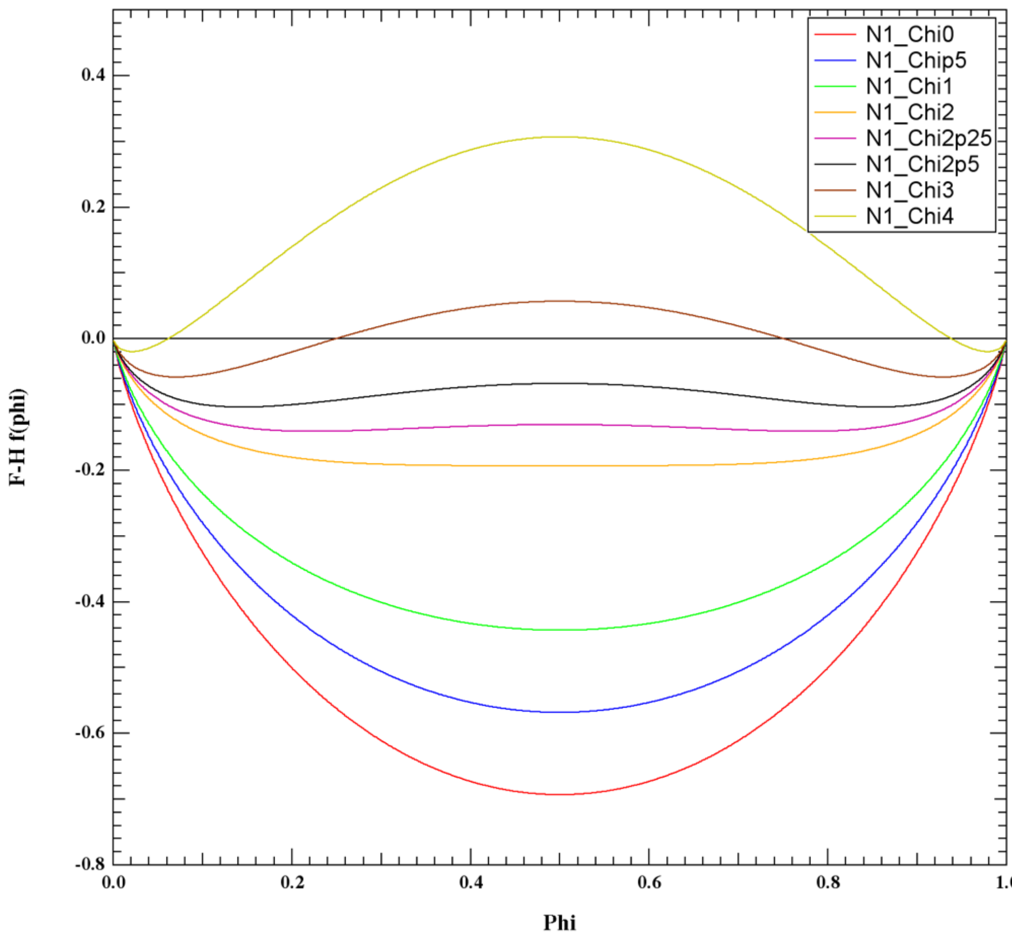

**Single Phase
to Critical
to Two Phase Regime
as Temperature Drops
(chi increases)**

Flor Huggins Equation for Polymer Blends

$$\frac{\Delta G}{kT} = \frac{\phi_A}{N_A}\ln(\phi_A) + \frac{\phi_B}{N_B}\ln(\phi_B) + \phi_A \phi_B \chi_{AB}$$

ΔG Free energy difference in going from separate polymers to mixed polymers
Φ_A Volume Fraction of polymer A
N_A Degree of polymerization (molecular weight/monomer molecular weight) of polymer A
χ_{AB} Average interaction between A and B chain units ~ 1/Temperature.

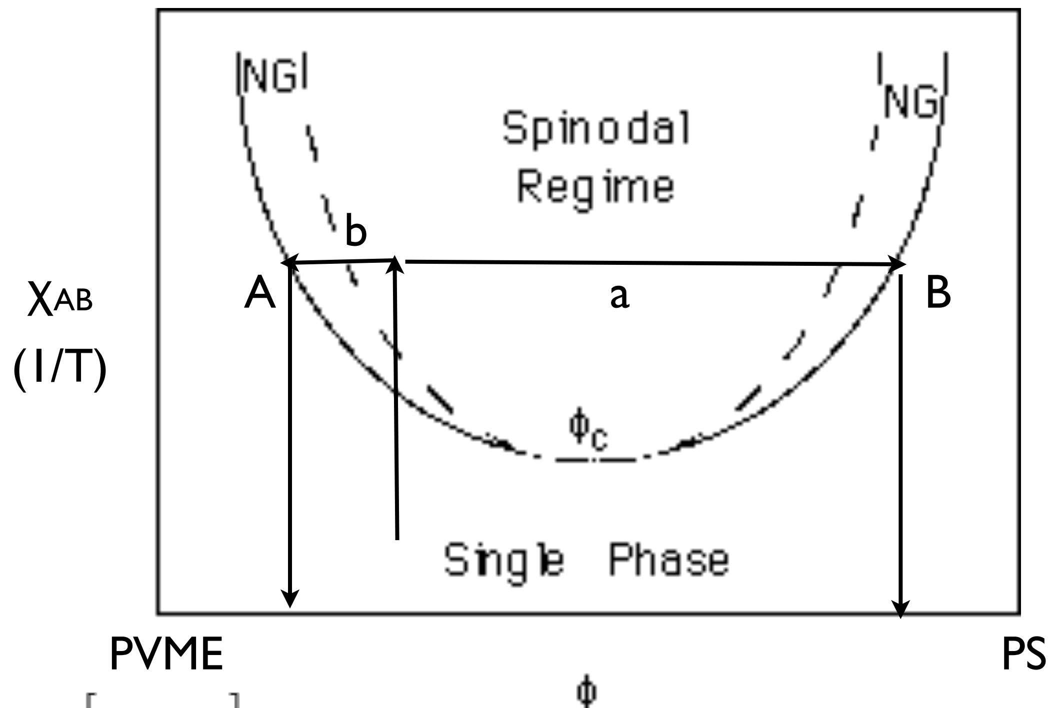

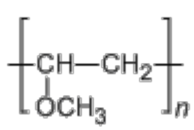

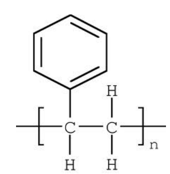

Tie Line

Equilibrium Composition
Determined by Binodal

Amount of Phase Determined by
Lever Rule (a with A; b with B)

Flor Huggins Equation for Polymer Blends

$$\frac{\Delta G}{kT} = \frac{\phi_A}{N_A}\ln(\phi_A) + \frac{\phi_B}{N_B}\ln(\phi_B) + \phi_A\phi_B\chi_{AB}$$

ΔG Free energy difference in going from separate polymers to mixed polymers
Φ_A Volume Fraction of polymer A
N_A Degree of polymerization (molecular weight/monomer molecular weight) of polymer A
χ_{AB} Average interaction between A and B chain units ~ 1/Temperature.

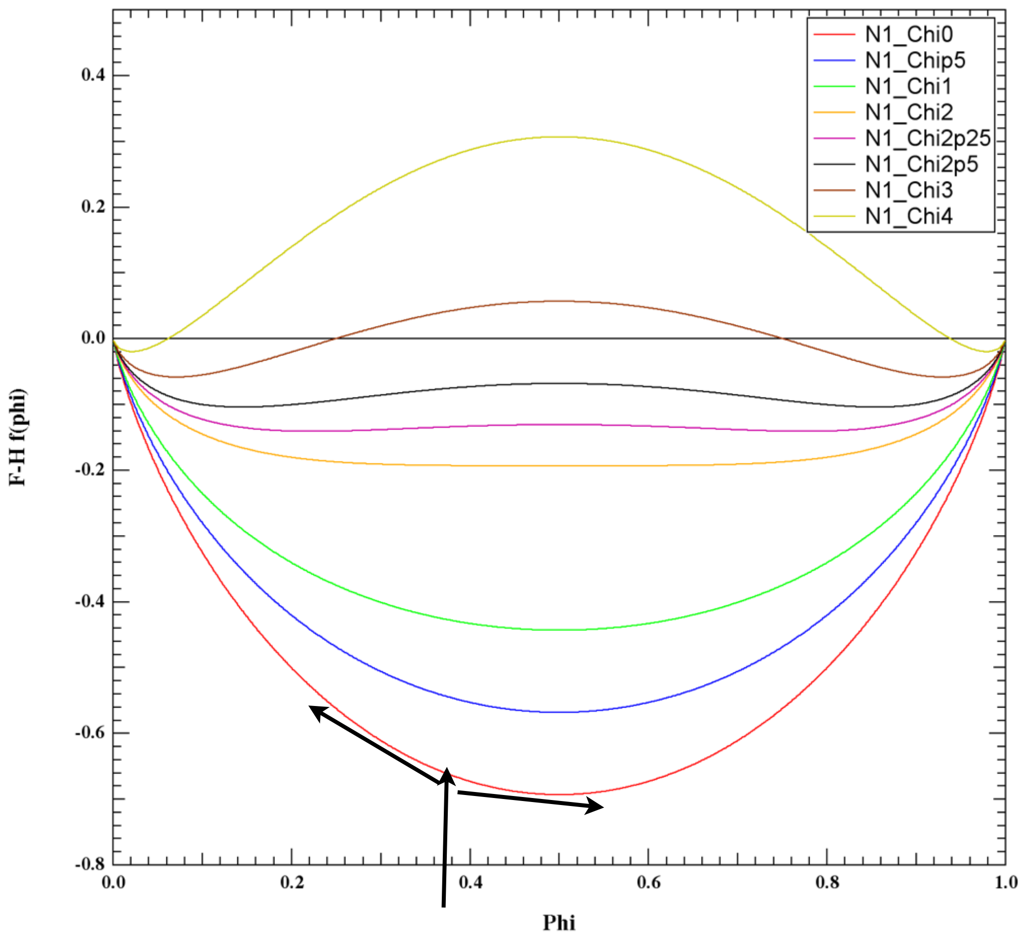

For Single Phase Every Attempt to Separate is Up Hill on Average

Flor Huggins Equation for Polymer Blends

$$\frac{\Delta G}{kT} = \frac{\phi_A}{N_A}\ln(\phi_A) + \frac{\phi_B}{N_B}\ln(\phi_B) + \phi_A\phi_B\chi_{AB}$$

ΔG Free energy difference in going from separate polymers to mixed polymers
Φ_A Volume Fraction of polymer A
N_A Degree of polymerization (molecular weight/monomer molecular weight) of polymer A
χ_{AB} Average interaction between A and B chain units ~ 1/Temperature.

Phase Diagram

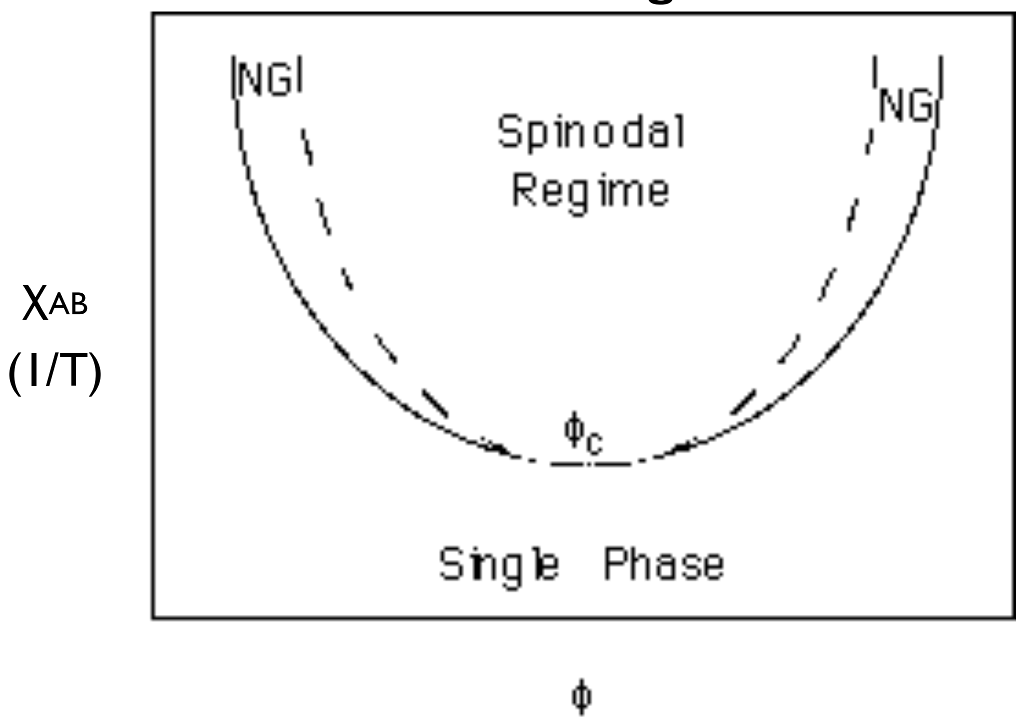

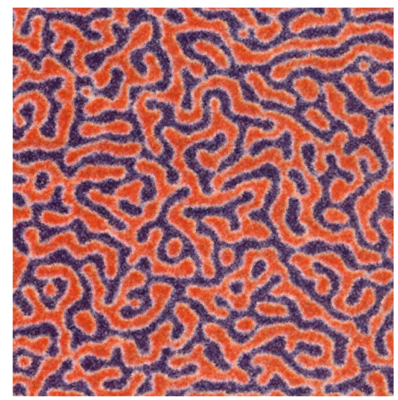

Simulation of pattern formed by spinodal decomposition in real space.

Spinodal Decomposition

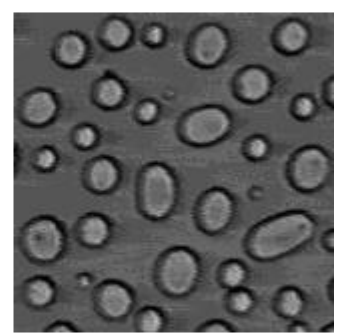

Nucleation and Growth

For Metals/Ceramics
We do not Usually Consider Liquid/Liquid Phase Separation
Consider Crystallization From a Liquid Phase

Isomorphous Phase Diagram

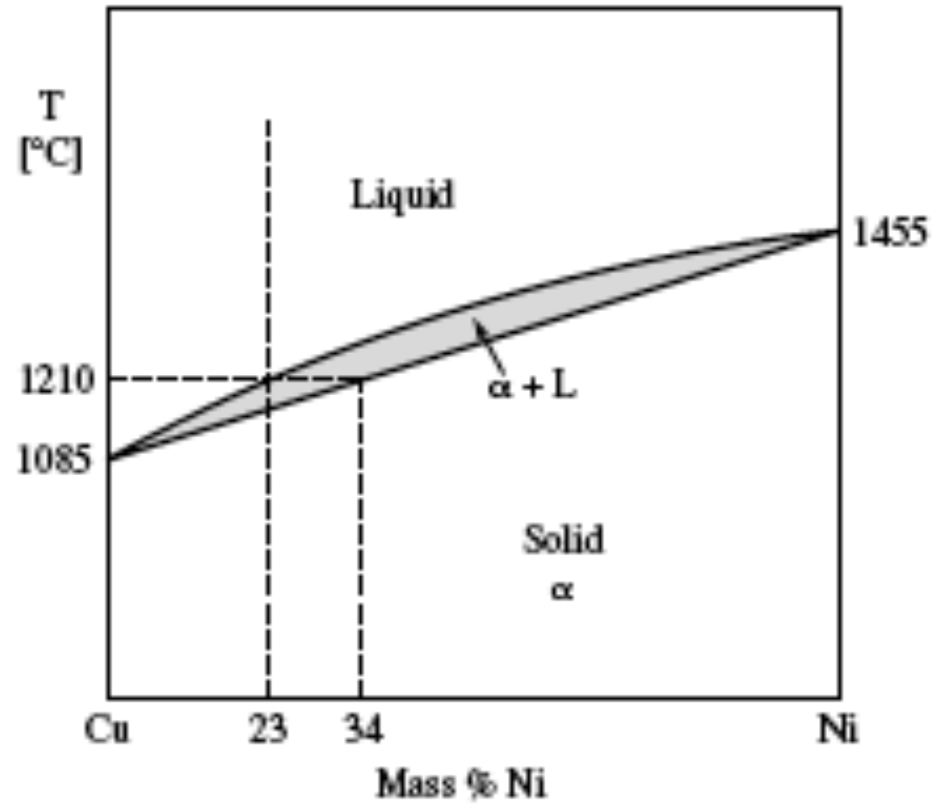

FIGURE 5.3. Copper–nickel isomorphous binary phase diagram. The composition here is given in mass percent (formerly called weight percent) in contrast to atomic percent. This section uses exclusively mass percent. For simplicity, the latter is generally designated as %.

Gibbs Phase Rule

Degrees of Freedom = Components - Phases + 2 or 1 (T & P)

1 2 2 1

For Metals/Ceramics
We do not Usually Consider Liquid/Liquid Phase Separation
Consider Crystallization From a Liquid Phase

Liquidus

and

Solidus

Lines

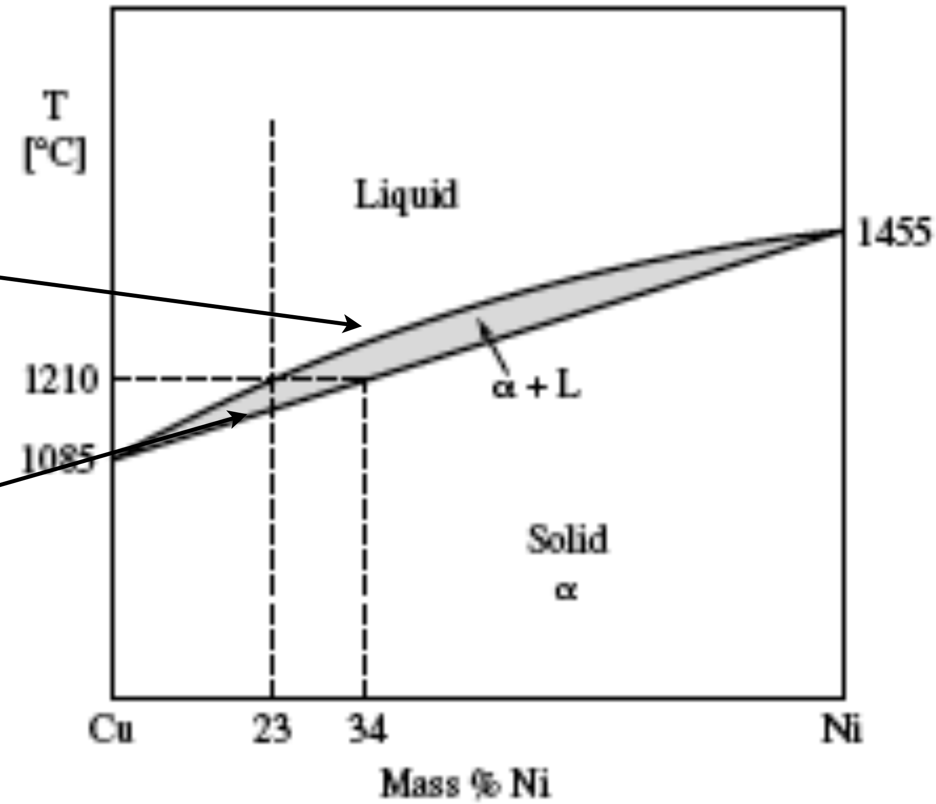

Gibbs Phase Rule

Degrees of Freedom = Components - Phases + 2 or 1 (T & P)

1 2 2 1

For Metals/Ceramics
We do not Usually Consider Liquid/Liquid Phase Separation
Consider Crystallization From a Liquid Phase

In the two phase regime
if you pick temperature
The composition of
the liquid and soid phases are fixed
by the tie line

If you pick the composition
of the liquid or solid phase
the temperature is fixed
by the tie line

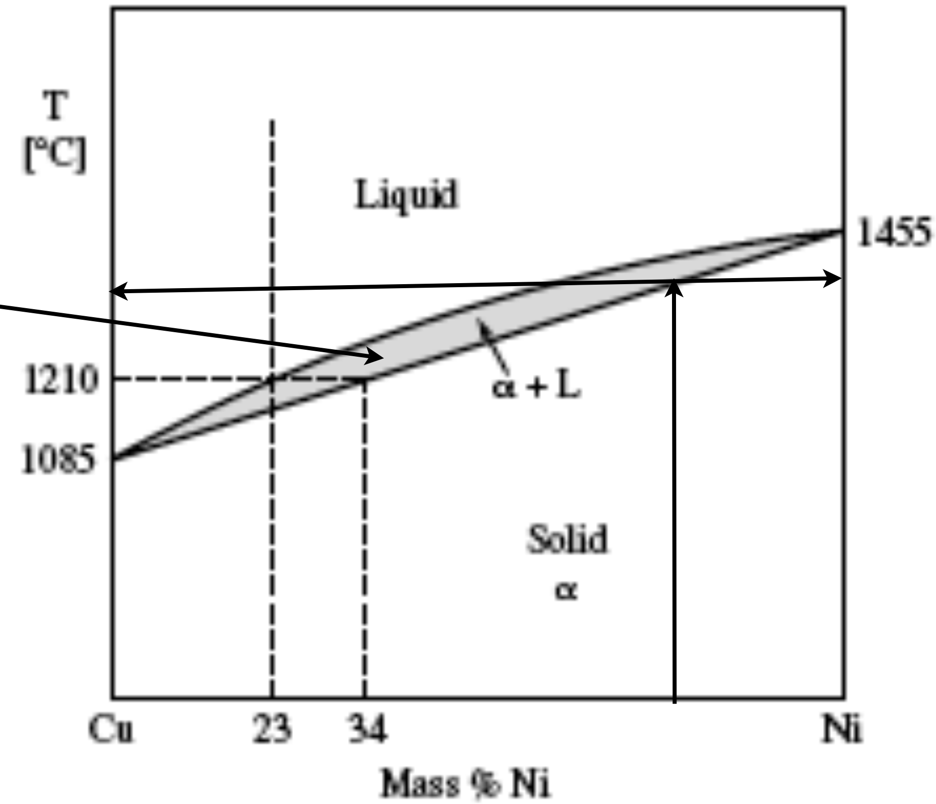

Gibbs Phase Rule

Degrees of Freedom = Components - Phases + 2 or 1 (T & P)

1 2 2 1

Substitutional Solid Solution

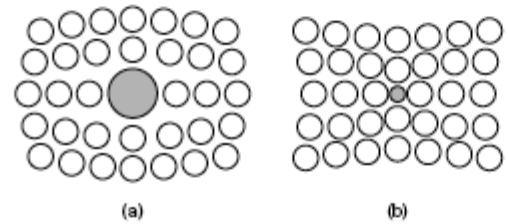

FIGURE 5.2. Distortion of a lattice by inserting (a) a larger (such as Sn) and (b) a smaller (such as Be) substitutional atom into a Cu matrix. The distortions are exaggerated.

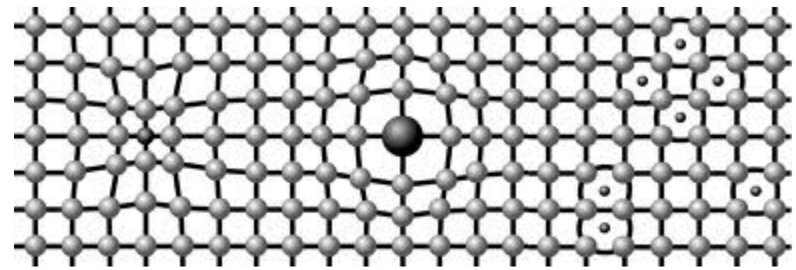

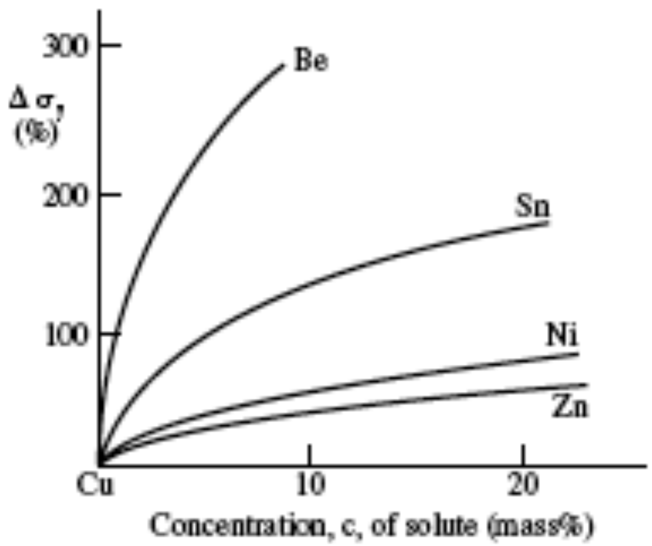

Hummel

FIGURE 5.1. Change in yield strength due to adding various elements to copper. The yield strength, σ_y, increases parabolically with the solute concentration.

Solid solution strengthening

Disclinations are trapped by lattice strain near larger or smaller substitutional atoms

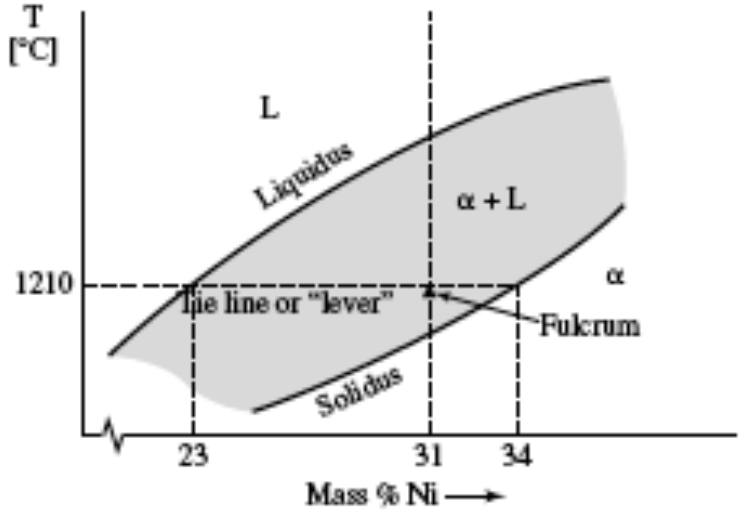

Hummel

FIGURE 5.4. Part of the Cu–Ni phase diagram to demonstrate the lever rule. The section of the lever between the fulcrum and the solidus line represents the amount of liquid. (The analogue is true for the other part of the lever.)

Thermodynamic Equilibrium

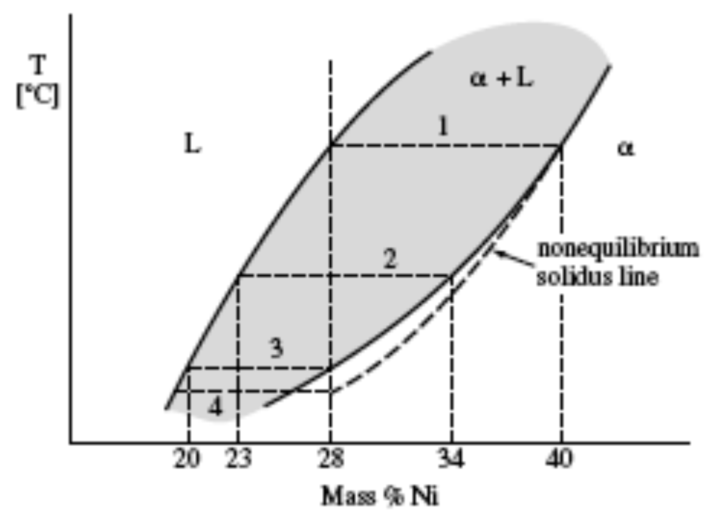

Hummel

FIGURE 5.5. Equilibrium (solid lines) and nonequilibrium (dashed line) solidus curve in a part of the Cu–Ni binary phase diagram.

Kinetics

Dendritic Growth

Crystalline growth occurs at different rates for different crystallographic directions so there is a preferred direction of growth

Growth can involve exclusion of impurities and transport of impurities from a "clean" crystal to the "dirty" melt

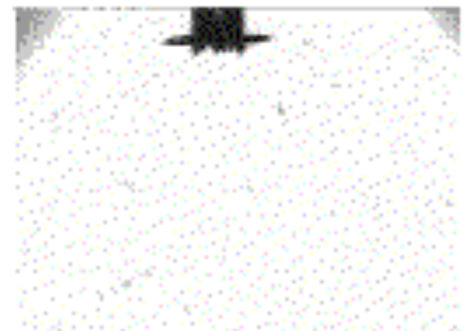

Crystallization releases energy so the temperature near a growth front can be too high for crystallization to occur. The melt can be colder and more likely to crystallize

Temperature differentials and the "kinetic" phase diagram can lead to segregation or coring as described by Hummel

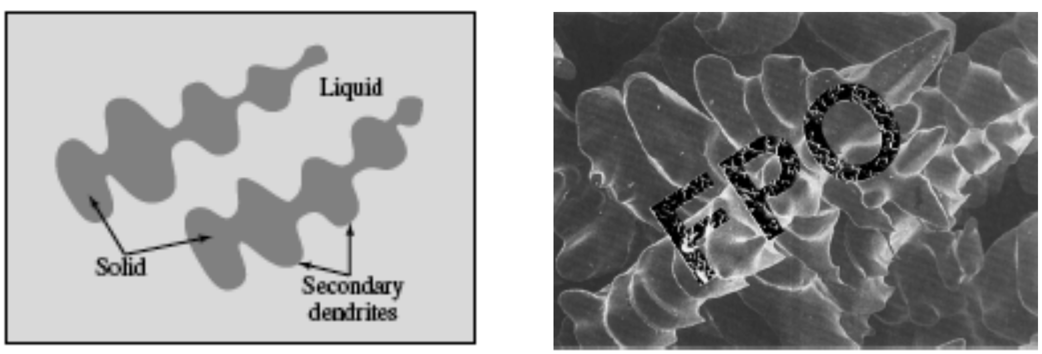

FIGURE 5.6. Microstructure of an alloy revealing dendrites: (a) schematic, (b) photomicrograph of a nickel-based superalloy.

Callister p. 294

Figure 9.4 Schematic representation of the development of microstructure during the equilibrium solidification of a 35 wt% Ni–65 wt% Cu alloy.

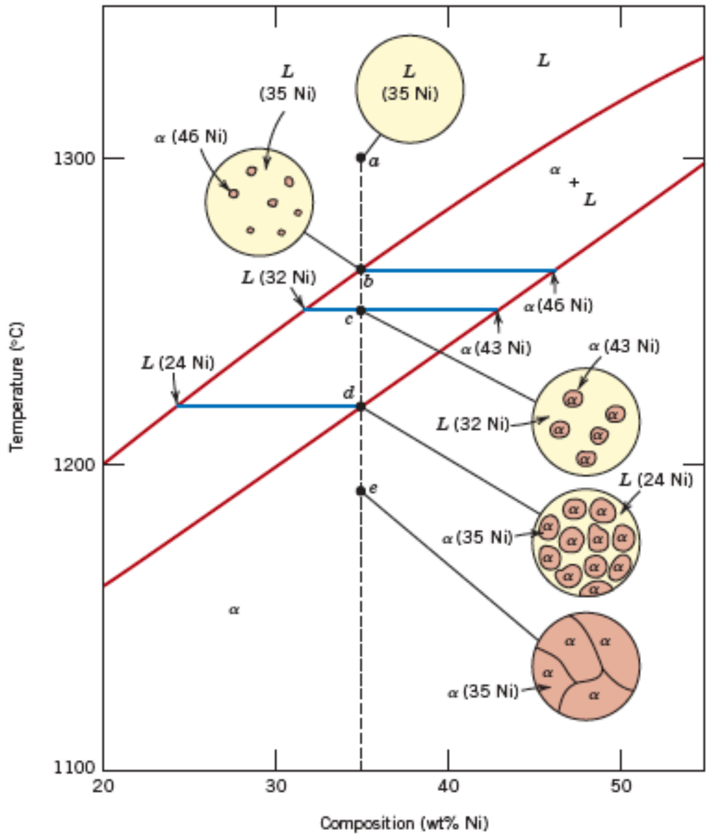

Figure 9.5 Schematic representation of the development of microstructure during the nonequilibrium solidification of a 35 wt% Ni–65 wt% Cu alloy.

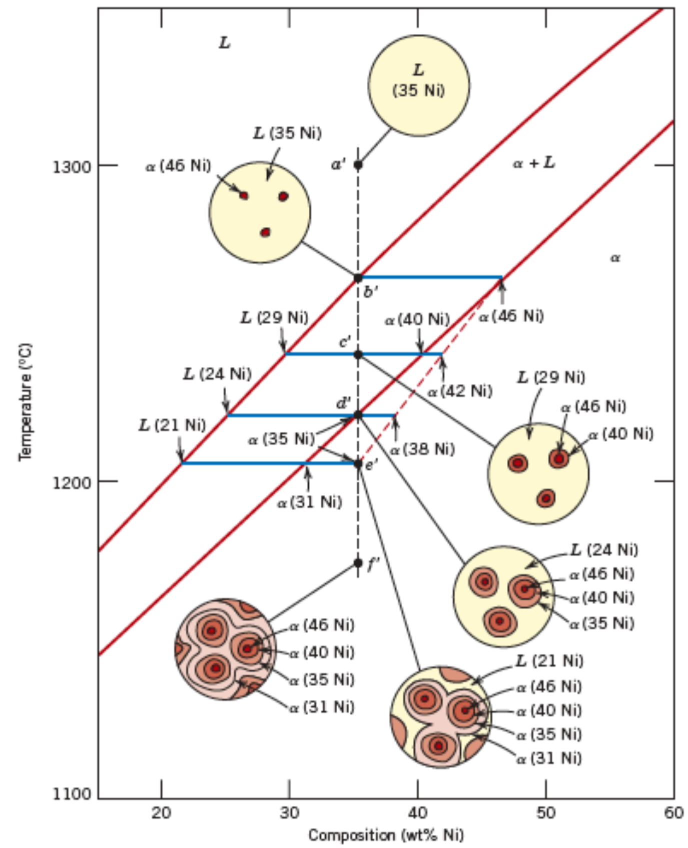

Equilibrium

Non-Equilibrium

Mechanical Properties of Isomorphous Binary Alloy

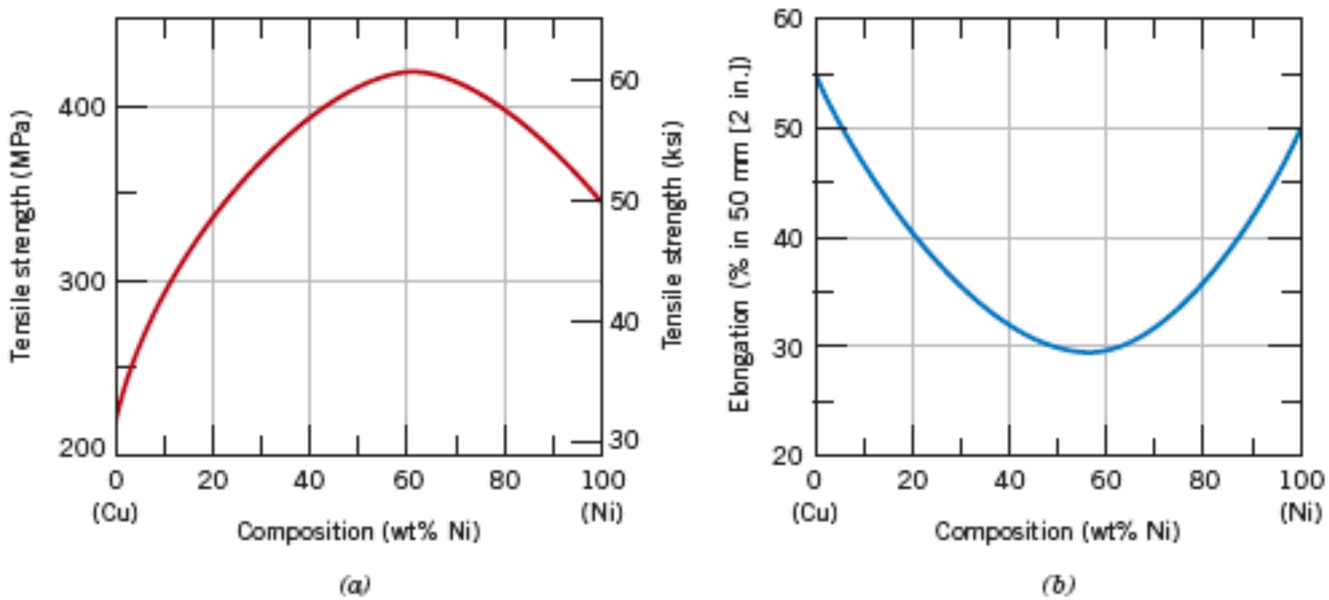

Figure 9.6 For the copper–nickel system, (*a*) tensile strength versus composition, and (*b*) ductility (%EL) versus composition at room temperature. A solid solution exists over all compositions for this system.

Types of Phase Diagrams

2 Phases
Isomorphous

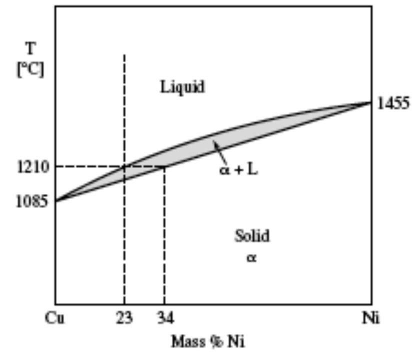

3 Phases
Eutectic

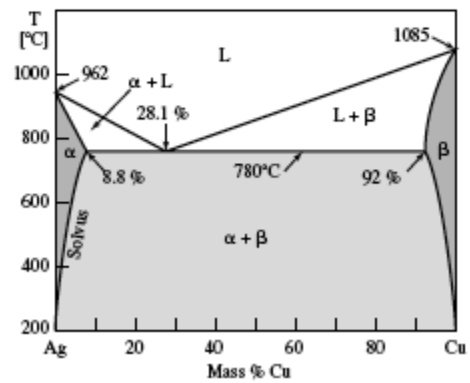

Eutectoid

Peritectic

Peritectoid

Monotectic

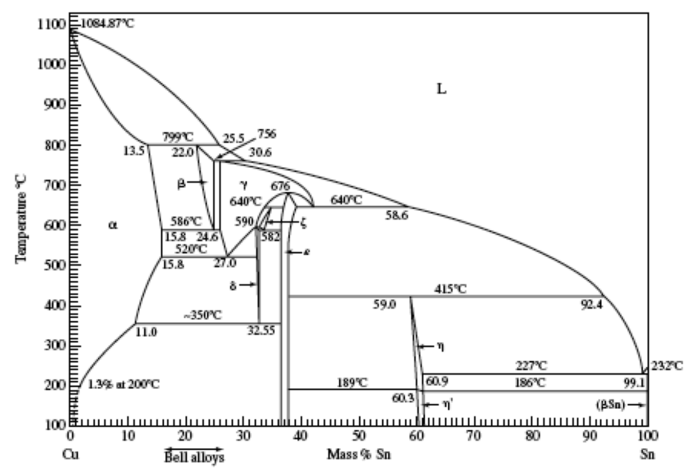

Monotectoid

Degrees of Freedom = Components - Phases + 1

1 phase => 2 DOF (T & Comp)
2 phase => 1 DOF
3 phase => 0 DOF

Eutectic Phase Diagram

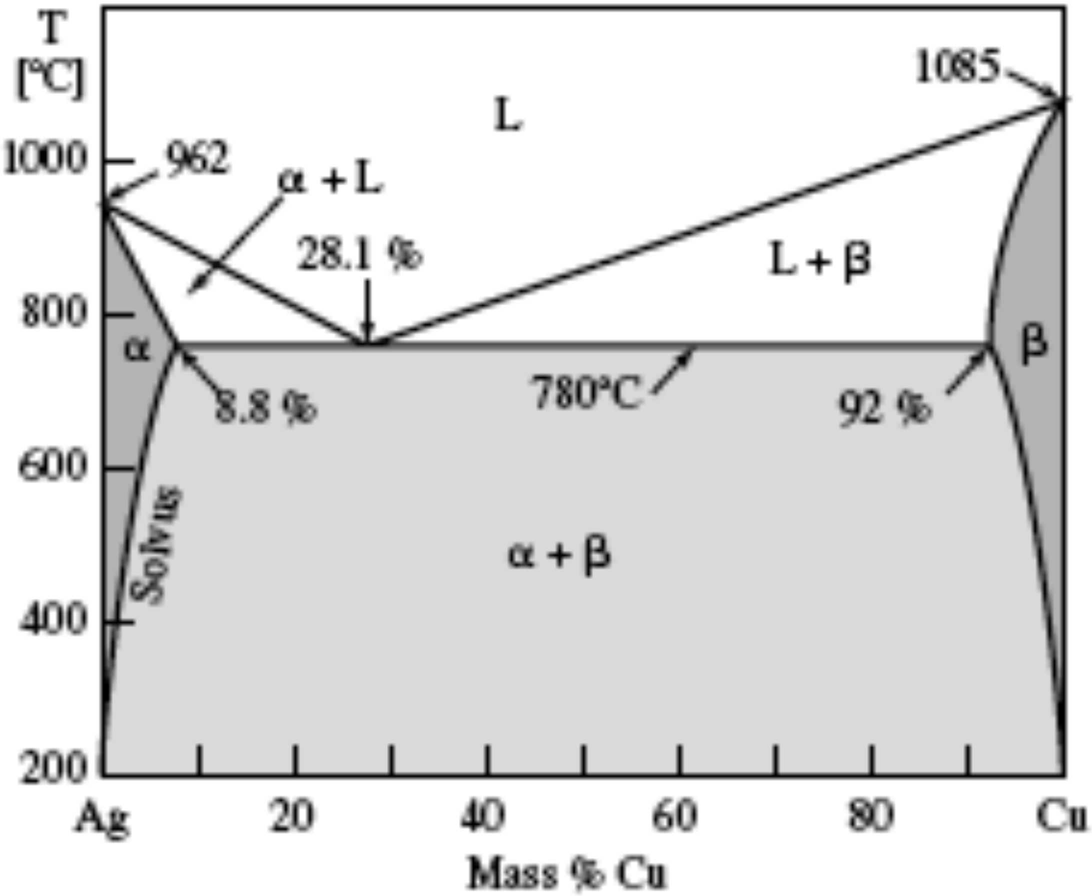

$L_{28.1\%\ Cu} \rightarrow \alpha_{8.8\%\ Cu} + \beta_{92\%\ Cu}$.

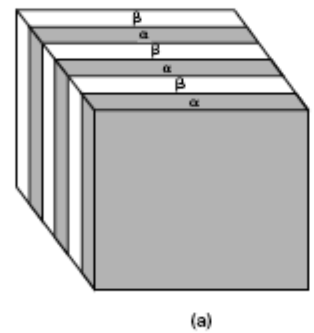

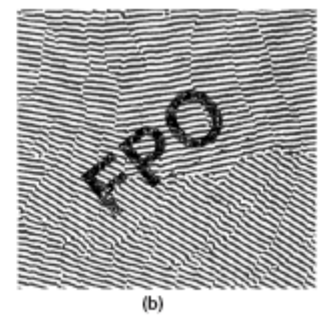

FIGURE 5.9. (a) Schematic representation of a lamellar or platelike microstructure as typically observed in eutectic alloys. (b) Photomicrograph of a eutectic alloy, 180× ($CuAl_2$–Al). Reprinted with permission from *Metals Handbook, 8th Edition*, Vol. 8 (1973), ASM International, Materials Park, OH, Figure 3104, p. 156.

FIGURE 5.7. Binary copper–silver phase diagram containing a eutectic transformation.

Degrees of Freedom = Components - Phases + 1

Figure 9.13 Schematic representations of the equilibrium microstructures for a lead–tin alloy of eutectic composition C_3 above and below the eutectic temperature.

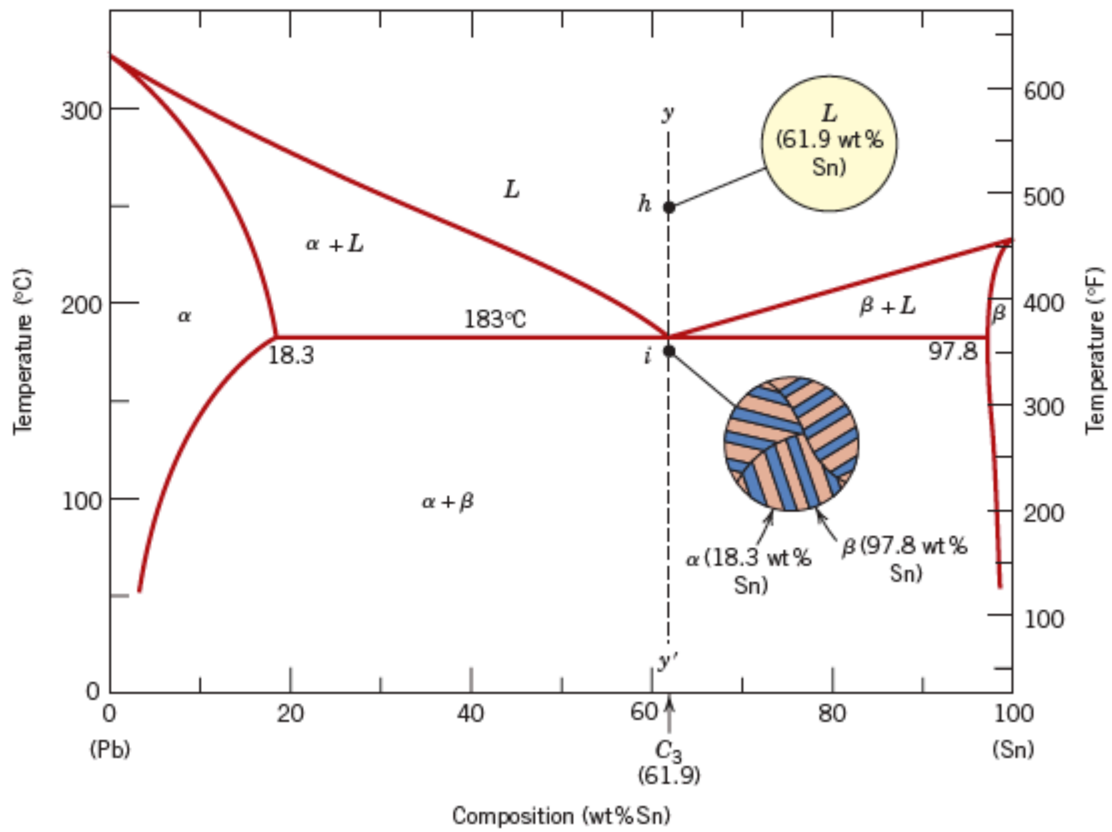

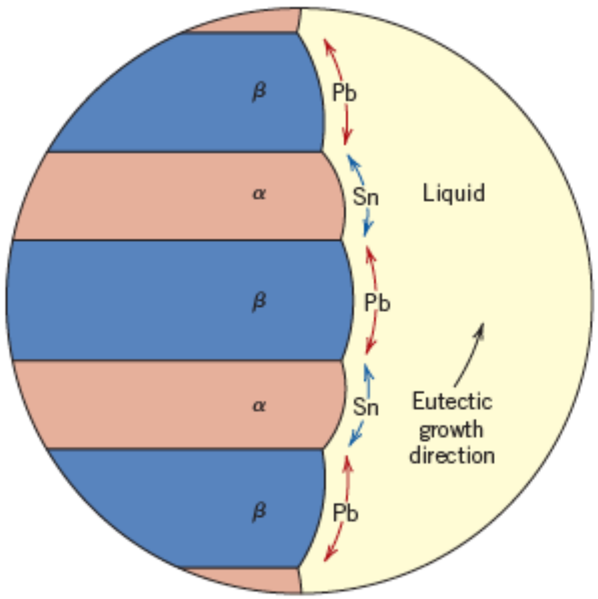

Figure 9.15 Schematic representation of the formation of the eutectic structure for the lead–tin system. Directions of diffusion of tin and lead atoms are indicated by blue and red arrows, respectively.

Eutectic Phase Diagram

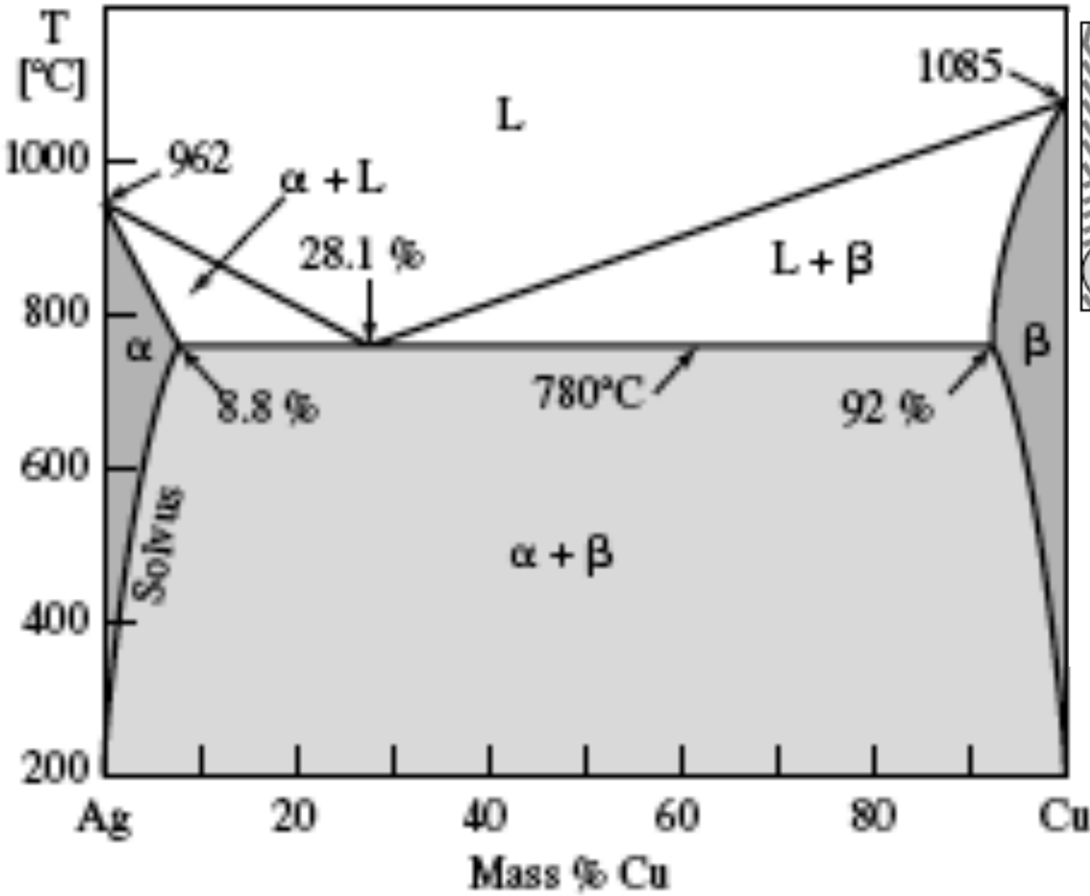

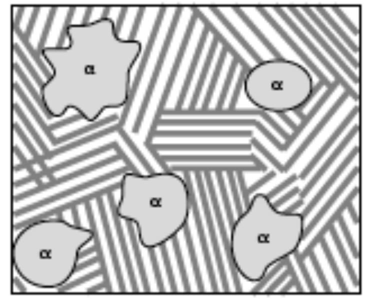

(a)

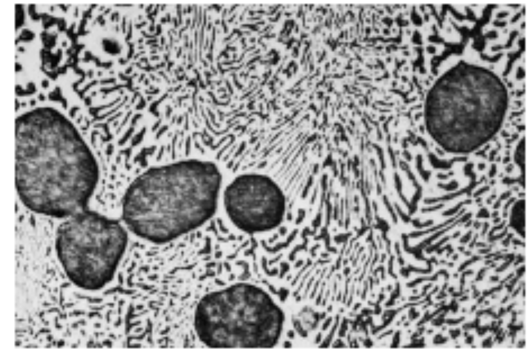

(b)

FIGURE 5.10. (a) Schematic representation of a microstructure of a hy-poeutectic alloy revealing primary α particles in a lamellar mixture of α and β microconstituents. (b) Microstructure of 50/50 Pb-Sn as slowly solidified. Dark dendritic grains of lead-rich solid solution in a matrix of lamellar eutectic consisting of tin-rich solid solution (white) and lead-rich solid solution (dark) 400×, etched in 1 part acetic acid, 1 part HNO_3, and 8 parts glycerol. Reprinted with permission from Metals Handbook, 8th Ed. Vol **7**, page 302, Figure 2508, ASM International, Materials Park, OH (1972).

FIGURE 5.7. Binary copper–silver phase diagram containing a eutectic transformation.

Degrees of Freedom = Components - Phases + 1

Hyper and Hypo Eutectic

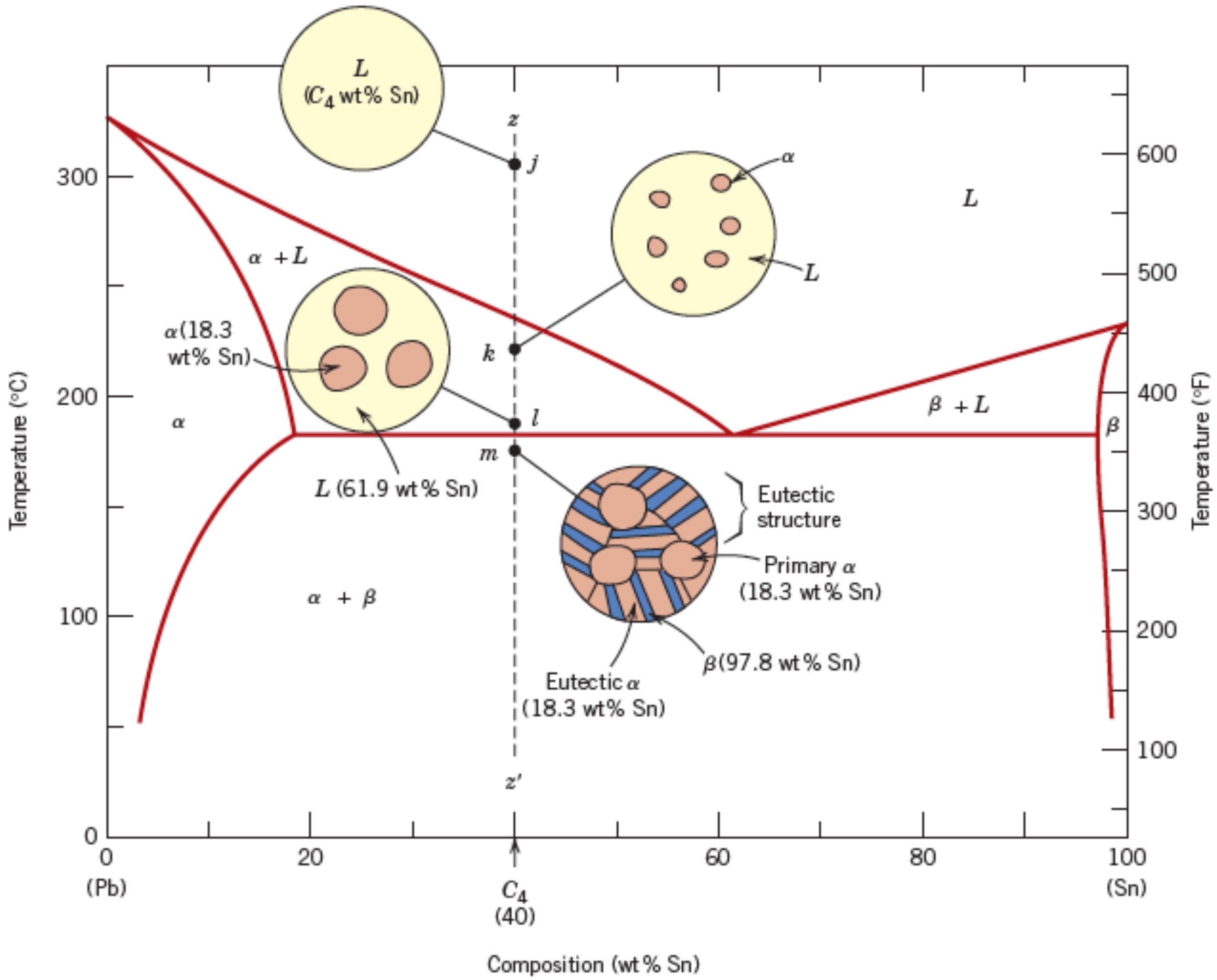

Figure 9.16 Schematic representations of the equilibrium microstructures for a lead–tin alloy of composition C_4 as it is cooled from the liquid-phase region.

FIGURE 5.8. Schematic representation of a cooling curve for a eutectic alloy (or for a pure metal). The curve is experimentally obtained by inserting a thermometer (or a thermocouple) into the liquid alloy and reading the temperature in periodic time intervals as the alloy cools.

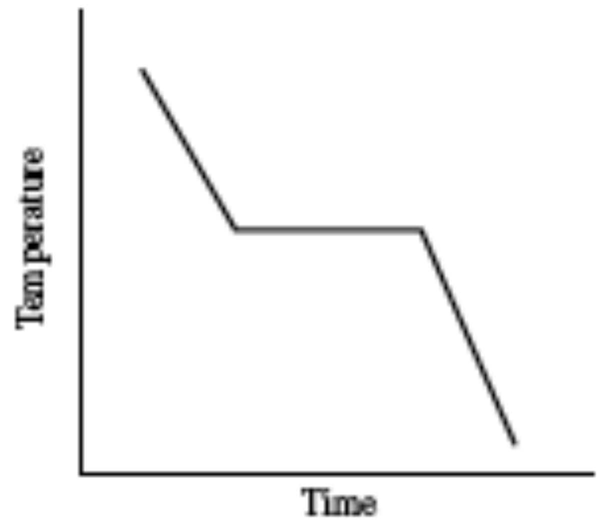

FIGURE 5.11. (a) Schematic representation of the cooling curve for a hypoeutectic alloy revealing the eutectic plateau (see Figure 5.8) and other characteristic landmarks as indicated. (b) Cooling curve for an isomorphous alloy (see Figure 5.3).

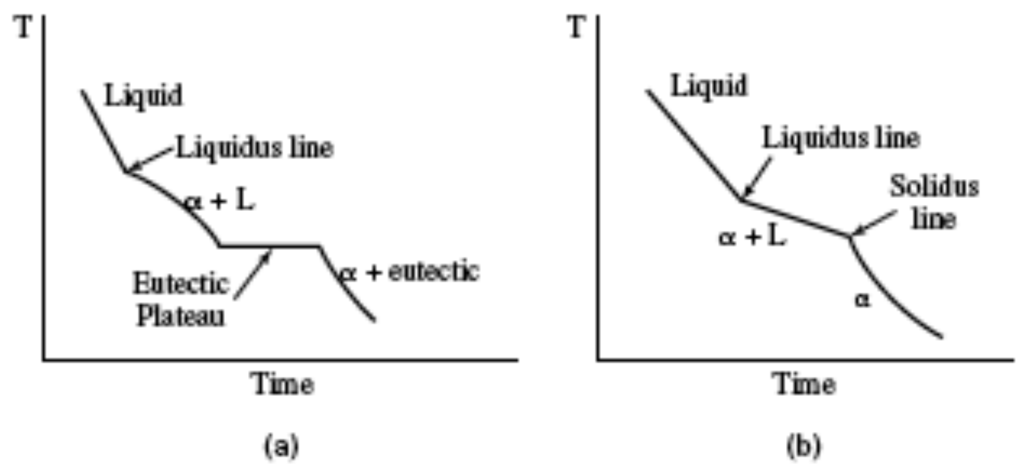

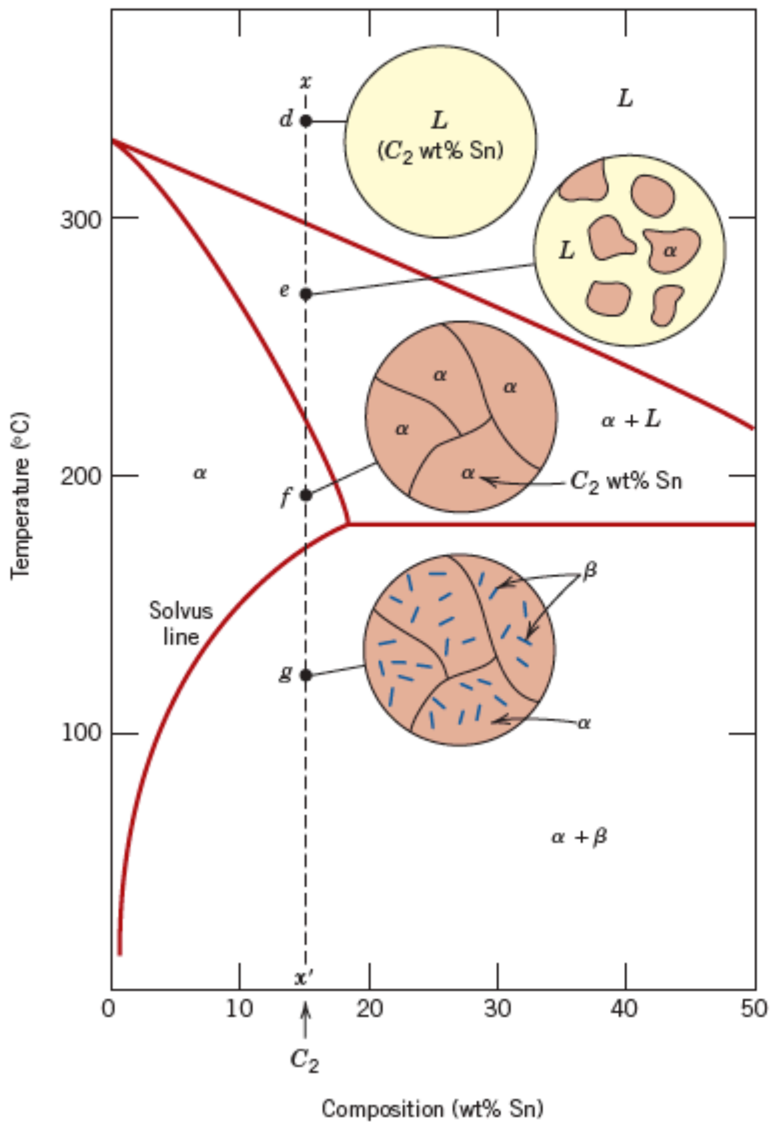

Figure 9.12 Schematic representations of the equilibrium microstructures for a lead–tin alloy of composition C_2 as it is cooled from the liquid-phase region.

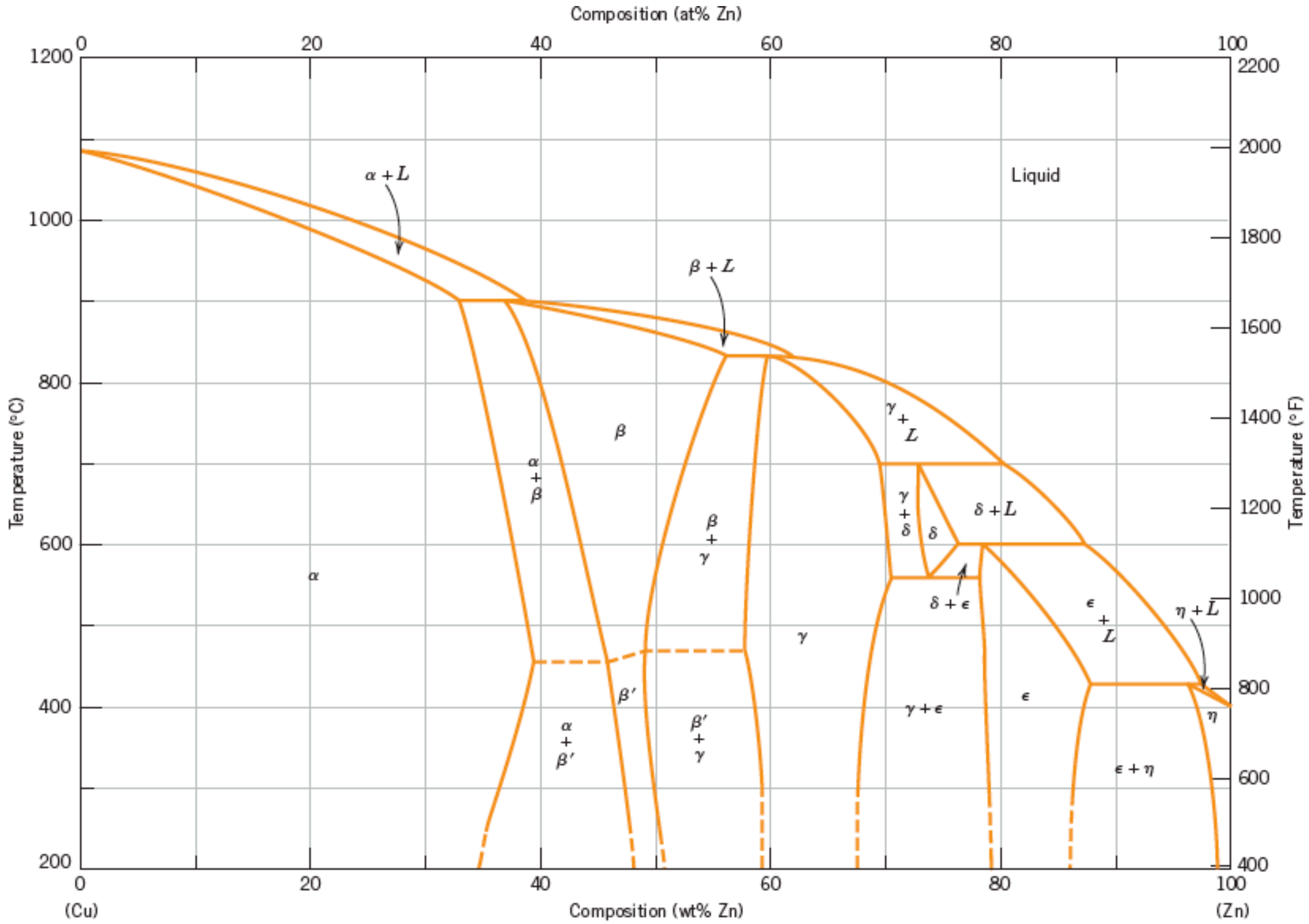

Figure 9.19 The copper–zinc phase diagram. [Adapted from *Binary Alloy Phase Diagrams,* 2nd edition, Vol. 2, T. B. Massalski (Editor-in-Chief), 1990. Reprinted by permission of ASM International, Materials Park, OH.]

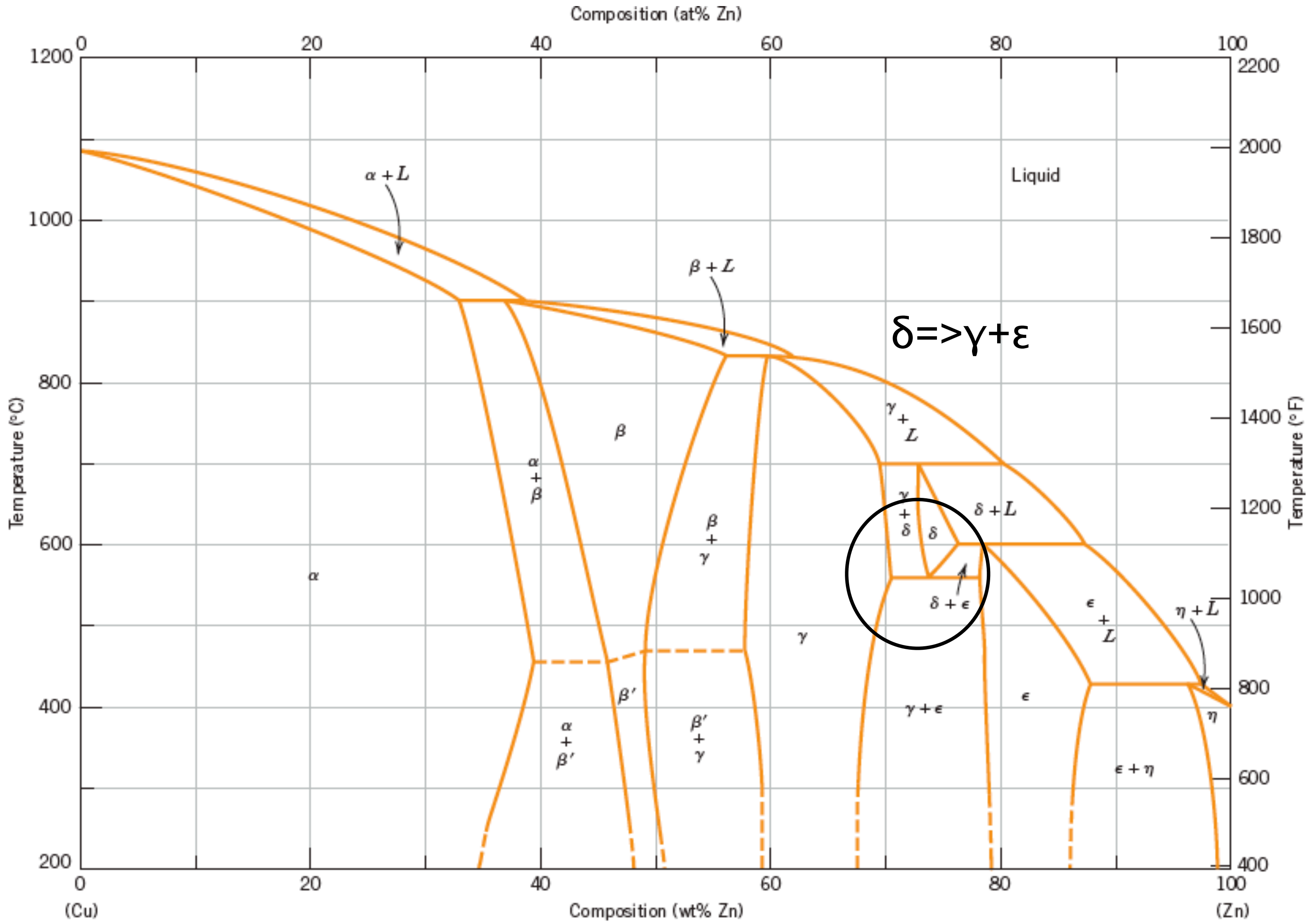

Figure 9.19 The copper–zinc phase diagram. [Adapted from *Binary Alloy Phase Diagrams,* 2nd edition, Vol. 2, T. B. Massalski (Editor-in-Chief), 1990. Reprinted by permission of ASM International, Materials Park, OH.]

Eutectoid

Eutectic L => α+β

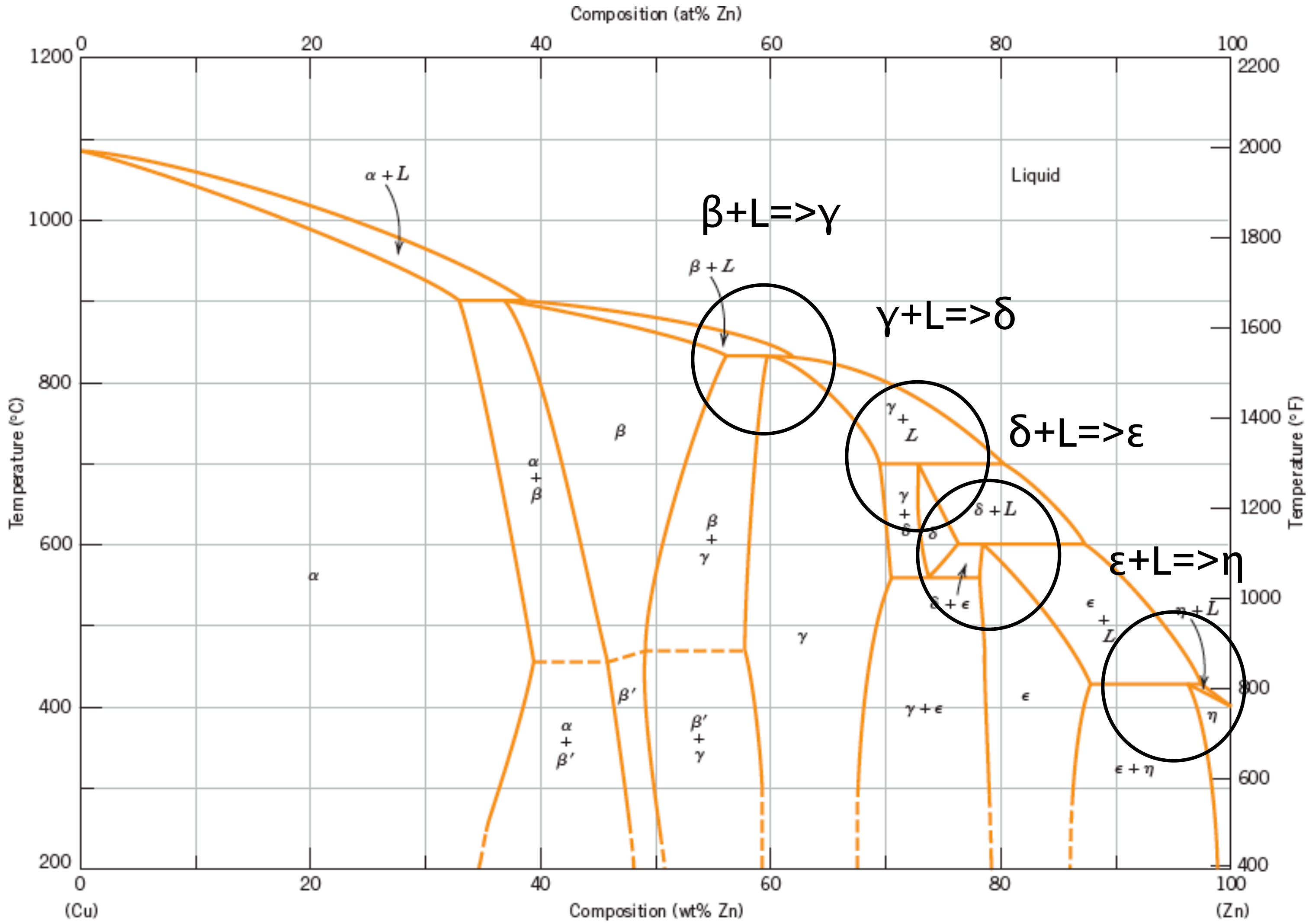

Figure 9.19 The copper–zinc phase diagram. [Adapted from *Binary Alloy Phase Diagrams,* 2nd edition, Vol. 2, T. B. Massalski (Editor-in-Chief), 1990. Reprinted by permission of ASM International, Materials Park, OH.]

Peritectic

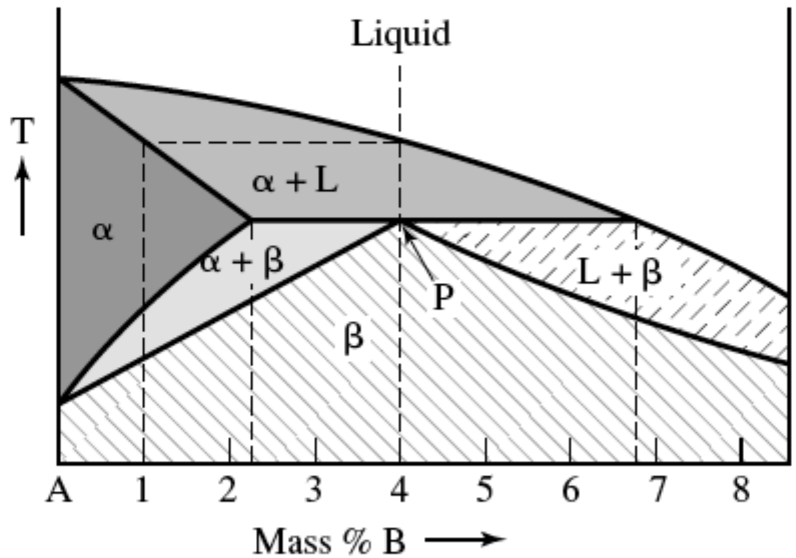

FIGURE 5.13. Part of a hypothetical phase diagram that contains a peritectic reaction.

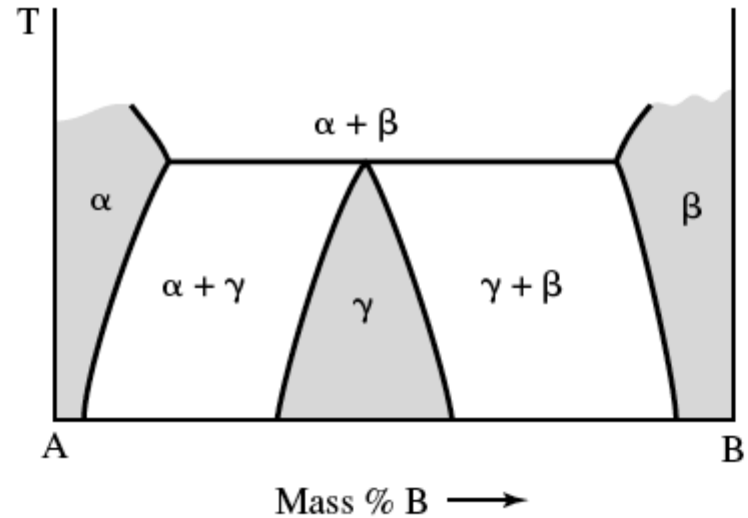

FIGURE 5.14. Schematic representation of a peritectoid reaction. The region at higher temperatures is not shown for clarity.

Monotectic $L_1 \Rightarrow L_2 + \alpha$

Monotectoid $\alpha_1 \Rightarrow \alpha_2 + \gamma$

Peritectic $\beta + L \Rightarrow \gamma$

Peritectoid $\beta + \gamma \Rightarrow \varepsilon$

Eutectic $L \Rightarrow \alpha + \beta$

Eutectoid $\beta \Rightarrow \gamma + \varepsilon$

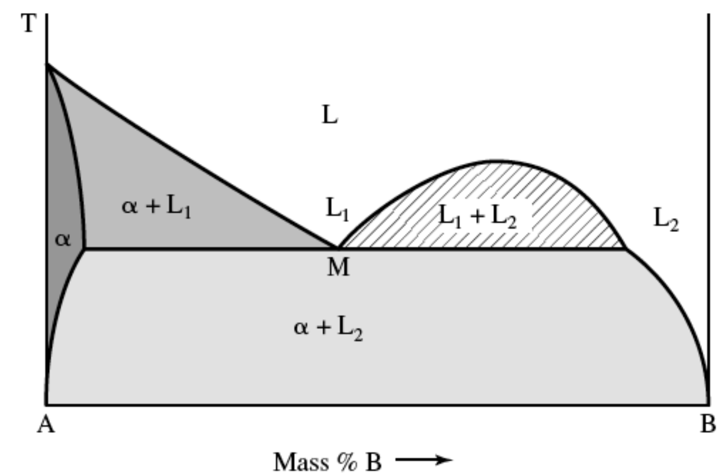

FIGURE 5.15. Schematic representation of a miscibility gap in the liquid state causing a monotectic reaction as given in Eq. (5.6).

Intermetallic

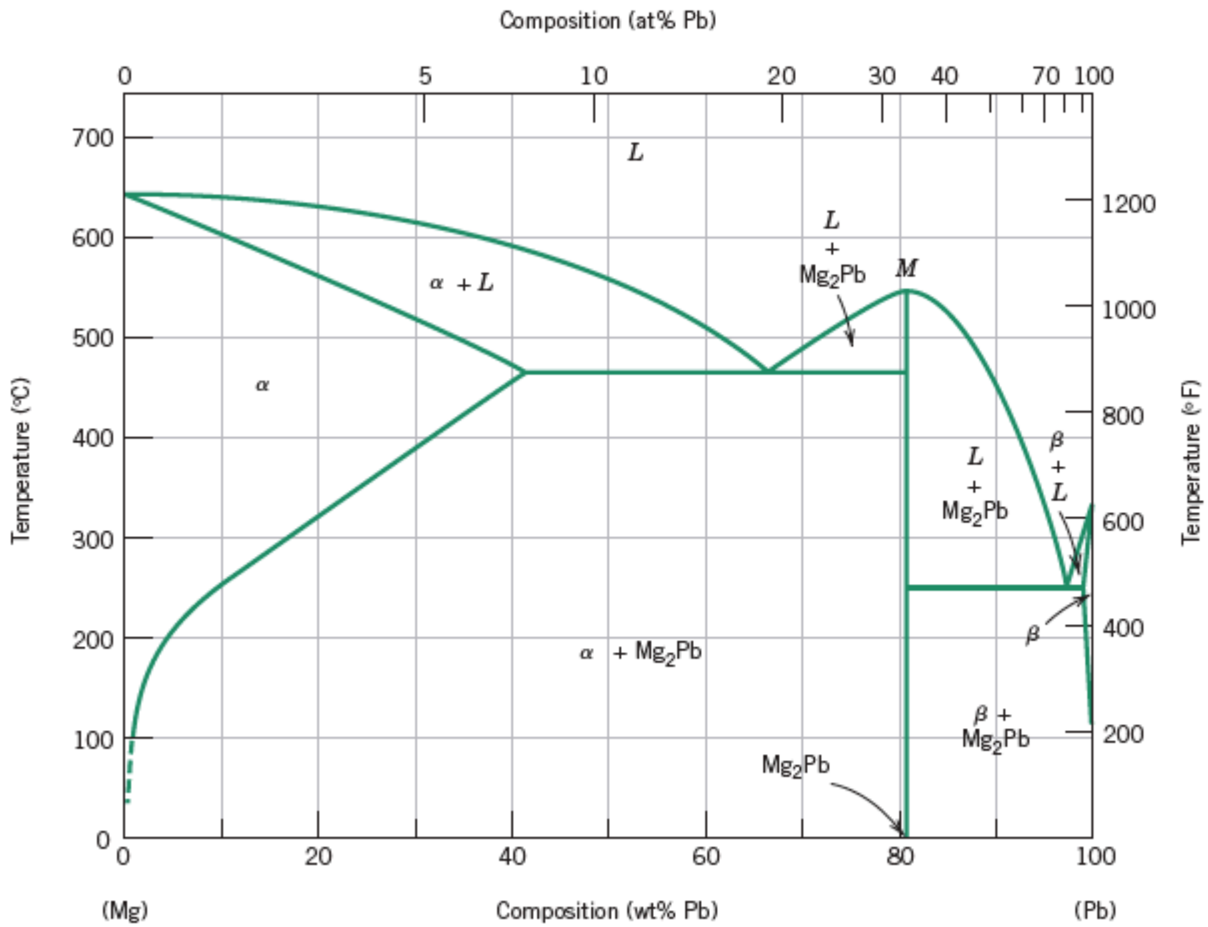

Figure 9.20 The magnesium–lead phase diagram. [Adapted from *Phase Diagrams of Binary Magnesium Alloys*, A. A. Nayeb-Hashemi and J. B. Clark (Editors), 1988. Reprinted by permission of ASM International, Materials Park, OH.]

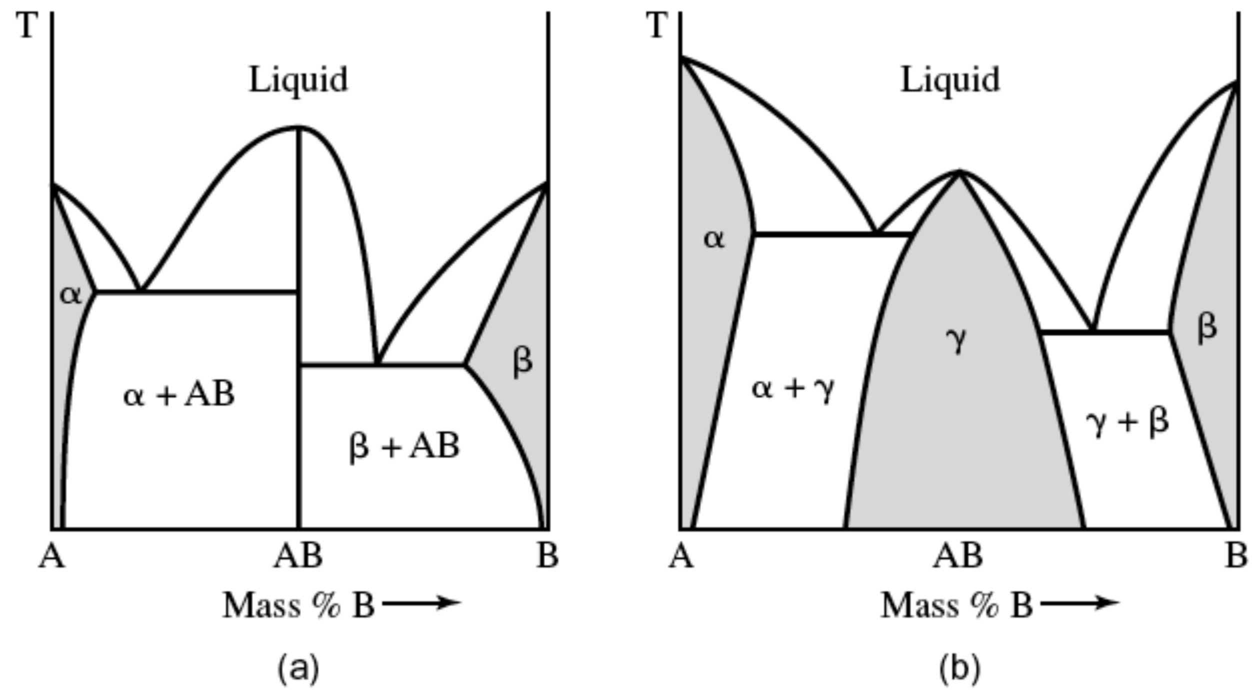

FIGURE 5.16. Schematic representation of (a) stoichiometric and (b) nonstoichiometric intermediate phases.

Iron/Carbon Phase Diagram

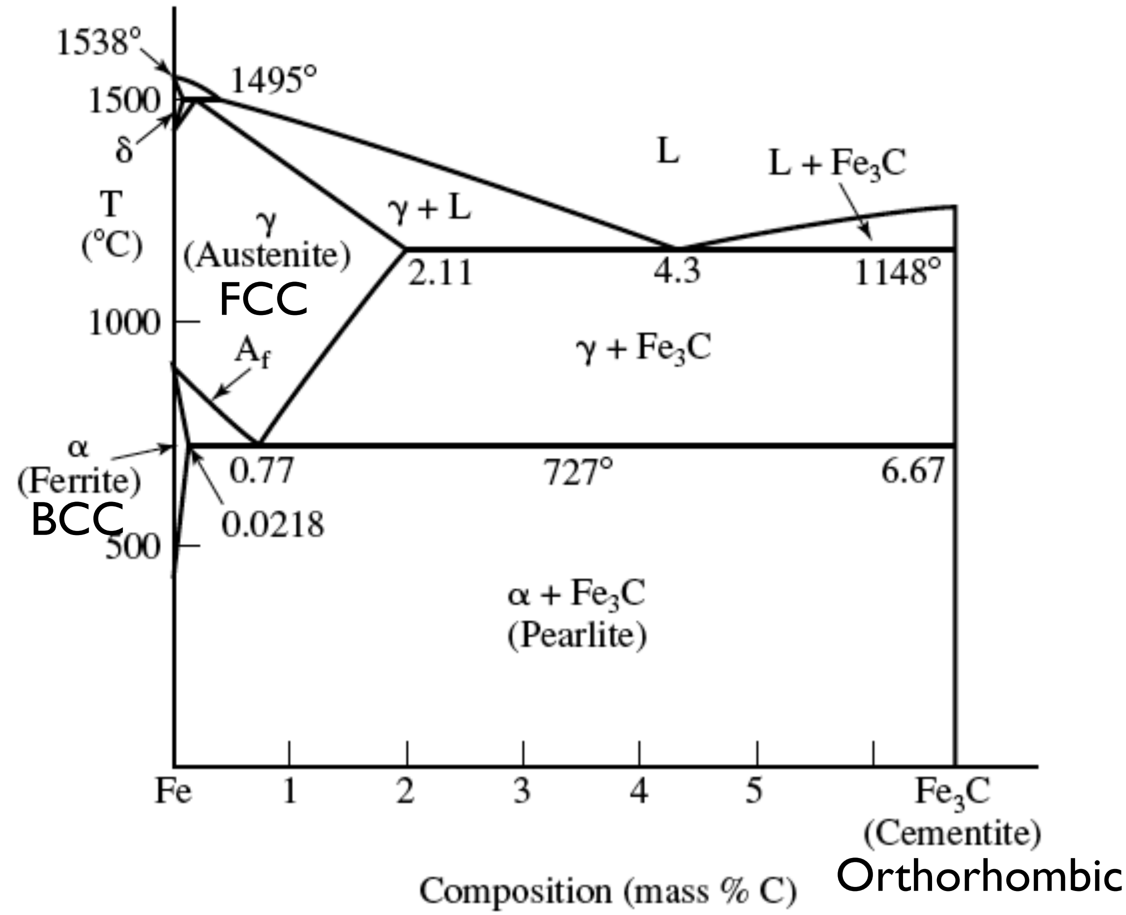

FIGURE 8.1. Portion of the iron–carbon phase diagram. (Actually, this section is known by the name *Fe-Fe_3C phase diagram*.) A_f is the highest temperature at which ferrite can form. As before, the mass percent of solute addition is used (formerly called weight percent).

Martensite (non equilibrium BCT phase from quench of γ)